Response to the reviewers on the manuscript "Methane retrieved from TROPOMI: improvement of the data product and validation of the first two years of measurements" by Alba Lorente et al.

The authors would like to thank the reviewers for their thoughtful and helpful comments and suggestions. Below are the comments by the reviewers in blue and replies in black. Any modification made to the text has been underlined. The line and page numbers correspond to the version of the manuscript available for online discussion.

Reviewer 1

Comment C 1.1 — Page 1, line 2: I recommend to add "and sampling" after "spatial resolution" as TROPOMI has a similar spatial resolution as GOSAT but much denser spatial sampling.

Reply: Added. We have also been more specific on the sampling technique of GOSAT on page 6, line 4.

Comment C 1.2 — Page 1, line 5: "The updated TROPOMI CH4 product...": If possible, please add version number. Does this product exist, i.e., is it available for interested users? If not, then please write "The updated TROPOMI CH4 retrieval algorithm...".

Reply: It is an existing product and it is publicly available through the ftp specified in the "Data availability" section. However, as we do not want to confuse the reader with version numbers and detailed specifications about the product in the abstract, we have modified the sentence to "The updated retrieval algorithm..." as the features that follow in that sentence refer to the algorithm itself.

Comment C 1.3 — Page 2, line 24: Barre et al., 2020: Missing in section "References". Please add. Please add that there is (at least) one other product as described in Schneising et al., 2019, and Schneising et al., 2020. These publications need to be cited (see References below) and the results shown in Schneising et al., 2020, need to be mentioned, especially those related to the Permian basin (see line 22).

Reply: We have added Barre et al. (2020) to the reference list; this was forgotten because when preparing this manuscript it was still under discussion in ACPD.

We agree that the WFM-DOAS TROPOMI product (Schneising et al., 2019) should be mentioned. We have mentioned it in Section 2.1 (TROPOMI CH_4 retrieval algorithm), page 4, line 27. We think this location fits better as it is here where the retrieval algorithm is presented. The added

text is: "Another scientific retrieval algorithm using the Weighting Function Modified Differential Optical Absorption Spectroscopy (WFM-DOAS) method to retrieve CO and CH_4 from TROPOMI was presented by Schneising et al. (2019). Comparison of both retrieval approaches is foreseen as part of ongoing verification activities."

We have added Schneising et al. (2020) when we refer in the text to the studies of the Permian basin. We do not go into the details of neither Schneising et al. (2020) nor Zhang et al. (2020) as the aim of this paragraph is to highlight some of the studies that have successfully used TROPOMI XCH_4 data to derive emissions.

Comment C 1.4 — Page 4, line 15, and Eq. (4): Instrument noise is not the only contributor to "XCH4 random errors", i.e., precision, as also other instrumental (e.g., inhomogeneous scene illumination) and retrieval errors (e.g., unconsidered variability of albedo and aerosols) may contribute. I suggest to add this limitation or, alternative, state that Eq. (4) is the definition of precision as used for this manuscript.

We acknowledge that there are other contributions to the random error besides the measurement noise. So it is true that Eq. 4 is the definition of the precision given in the product and so as used for this manuscript. As suggested by the reviewer, we explicitly mention this. "The precision σ_{XCH_4} available in the data product is defined as the standard deviation of the retrieval noise".

Comment C 1.5 — Page 4, line 21: "In cases when VIIRS data is not available, we use a back-up...": Does this happen? If yes, I would expect that this results in inconsistencies. Please add more information.

Reply: Data from VIIRS is hardly ever not available, so this does not happen very often. VIIRS data used in the TROPOMI XCH_4 retrieval is processed operationally by the S5P-NPP cloud processor. If due to any circumstance the processing of the VIIRS data fails or it is delayed, we use this filtering as a back up option. The XCH_4 data is flagged accordingly (qa value downgraded to 0.4) to avoid any possible inconsistencies as mentioned by the reviewer. From all the orbits processed operationally since the beginning of the mission, for less than 1% the processing of VIIRS data was not nominal in the CH_4 retrieval.

We added the following to clarify this point: "In less than 1% of the cases when VIIRS data is not available, we use a back-up filter based on a non-scattering CH_4 retrieval from the weak and strong absorption bands (Hu et al., 2016). These cases are flagged accordingly by the quality value indicator."

Comment C 1.6 — Page 4, line 27 following: "This updated retrieval algorithm is referred to as the beta version of the TROPOMI XCH4 data product." Sentence not OK. An algorithm is not a data product.

Reply: We agree with the reviewer about the misleading terminology used here. We have modified the text as follows in page 4, line 27: "The TROPOMI XCH_4 scientific data product from SRON retrieved with the updated algorithm serves as a beta version of the operational processing."

Following this comment, we have further clarified at the beginning of Sect. 3 (page 6, line 20), removing the reference to version 1.3.0 that will eventually correspond to the future operational update but this is not certain as of now: "The TROPOMI XCH_4 scientific data product from SRON retrieved with the updated algorithm will be suggested for use in the operational processing in the next processor update.."

Comment C 1.7 — Below Tab. 1: "*For the Lauder station the ll instrument was replaced on October 2018 to ll.". ll replaced by ll?

Reply: We thank the referee for spotting the typo. The instrument "ll" (Sherlock et al., 2017) was replaced by "lr" (Pollard et al., 2019). We have corrected this.

Comment C 1.8 — Page 5, line 9: If the TROPOMI data are averaged daily then I assume that the TROPOMI XCH_4 averaging kernels have not been considered for the validation. Please add more info on this aspect.

Reply: The total column averaging kernel can only be used when CH_4 profile measurements with a high vertical resolution would be available for validation. However, the measurements from the TCCON network only provide total column integrated measurements which hampers the application of the averaging kernels.

Comment C 1.9 — Page 6, line 17: "both retrievals performed similarly": With respect to what? Likely not w.r.t. yield as number of data points in proxy product is much higher. Please refine the statement.

Reply: We agree with the reviewer that we should be more specific in this statement. We modify the text for that purpose: "...both retrievals performed similarly with respect to bias variability and precision when validating the retrieved XCH_4 with ground-based TCCON measurements. This study also concluded that both methods can retrieve XCH_4 in aerosol loaded scenes with retrieval errors of less than 1%."

Comment C 1.10 — Page 7, line 4: "and that retrieved aerosol parameters have realistic distributions". This is a strong (but unproven) statement. It needs to be shown in this paper that this is true.

Reply: We agree with the reviewer that this statement needs clarification. First, to avoid misinterpretation of the output of the retrieval to which we refer as "retrieved aerosols parameters",

we change the reference to them in the manuscript to "scattering parameters" instead of "aerosol parameters", and add the prefix *effective* ("effective aerosol distribution height", "effective size parameter" and "effective aerosol column"). With effective we want to highlight that these retrieved parameters are auxiliary parameters that characterize the scattering properties of the atmosphere in the radiative transfer model in the retrieval for which the target is XCH_4. The aerosol parameters are only effective ones but follow a distribution that we would expect, and that is what we meant by realistic distributions. We have modified the sentence in page 7, line 4:"[...] retrieved scattering parameters follow a distribution that we would expect".

Comment C 1.11 — Page 7, line 12: "19.7 ppb to 24.5 ppb": What does this mean? Is it a min to max range?

Reply: It refers to the reduction on the standard deviation of the differences mentioned at the beginning of the sentence. We add 'from', and correct the order because the reduction is from 24.5 to 19.7 ppb. Furthermore, there was a typo and 24.5 ppb is 21.5 ppb, which matches the 9% reduction specified in that same sentence.

Comment C 1.12 — Page 8, 6-7: "we have decided to use the SEOM-IAS spectroscopy database." I am not convinced. Was this a "political" decision? I conclude from Tab. 2 that HITRAN 2008 (used so far) is better. Is a slightly better fit quality (which can have many reasons in addition to spectroscopy) really a good argument if bias and scatter are getting larger?

Reply: We acknowledge that the text can be somewhat misleading. The "slightly" better fit quality refers to the results when looking only to retrievals around the TCCON stations. On a global scale (page 7, line 30) "we see that both the RMS and χ^2 improve significantly when using the SEOM-IAS database, with HITRAN 2008 giving the worst fitting results". The prove of this statement is not visually shown in the manuscript, but we have added the following to the text as suggested by Referee # 2 (comment 2.12): "Global mean χ^2 improves by 19% with SEOM-IAS cross-section and by 7% with HITRAN 2016 with respect to HITRAN 2008."

Figure R1 below shows the ratio of χ^2 of the retrieval with HITRAN 2008 and HITRAN 2016 (left) and HITRAN 2008 and SEOM-IAS (right), for one year of data averaged into daily 1° x 1° grid, which shows that SEOM-IAS cross section results in a significantly better χ^2 with respect to HITRAN 2008 and HITRAN 2016. In the sensitivity tests, the only parameter that changed in the retrieval was the spectroscopic database, so any difference in the retrieval results could be attributed to the different spectroscopy. From this we concluded (page 8, line 6) "In view of the better spectral fitting results in the retrieved XCH_4 we have decided to use the SEOM-IAS spectroscopy database".

Regarding the results shown in Table 2, it shows that each of the spectroscopic databases introduces an overall bias that cannot be used as an independent argument to favour a specific

database, as the comparison to GOSAT and TCCON might also be biased because of the specific spectroscopy used in their retrievals. The variation in the scatter of 1 to 3 ppb is not conclusive, as this is negligible if compared to the magnitude of other sensitivities and errors in the retrieval.

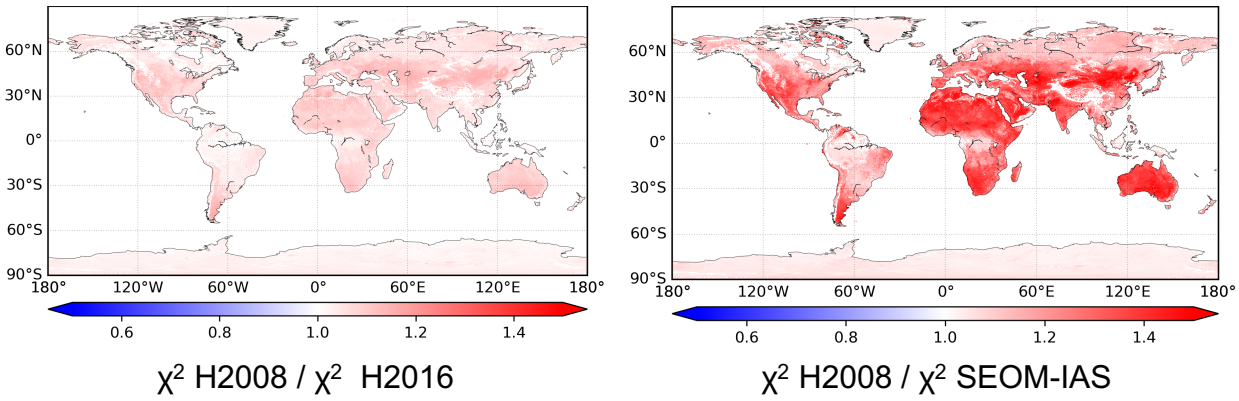

Figure R1: Ratio of χ^2 from the retrieval with HITRAN 2008 and HITRAN 2016 (left) and SEOM-IAS (right).

Comment C 1.13 — Section 3.4. Is this bias correction for albedo really new? As far as I know, the current operational XCH_4 product already offers a bias corrected product. Please clarify.

Reply: Indeed, the operational XCH_4 product already has a posteriori correction applied to it. The novelty of the bias correction presented in this study is the way we have derived it, as we have not used any external or reference data (like GOSAT or TCCON) to estimate the dependence, and the fit to the dependence on surface albedo is done differently.

The new approach is explained in page 10, line 10 – page 11, line 3. Also in page 11, line 19 we refer to the approach in the operational compared to the new fit: "for which the B-spline fit corrects more strongly than the regular polynomial fit that was previously used."

We try to make it clearer by modifying the text:

- Page 10, line 10: "In the baseline operational algorithm few months after TROPOMI was operational, we applied a correction..."

- Page 10, line 12: "[..] we have sufficient data to derive a new ~~the~~ correction".

Comment C 1.14 — Page 12, line 3: surface albedo "A_s": Is this the SWIR albedo? How is the NIR albedo considered?

Reply: In the correction we only consider the surface albedo in the SWIR spectral range, as the dependence of the bias on the surface albedo in the NIR spectral range (see Fig. R2) is negligible compared to the dependence shown in Fig. 3a for the surface albedo in the SWIR.

For clarification, we specify after Eq. 6 that A_s refers to the surface albedo in the SWIR, and in page 10, line 2: "The comparison of TROPOMI [...] shows a dependence of the bias [...] on surface albedo retrieved in the SWIR spectral range".

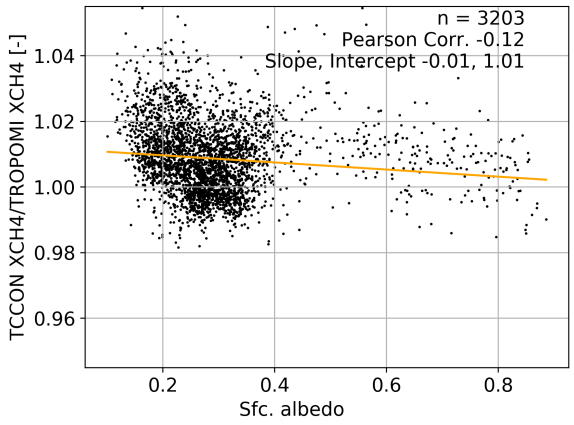

Figure R2: Ratio of XCH_4 measurements by TCCON and TROPOMI as a function of retrieved surface albedo in the NIR spectral range, to compare with Fig. 3a in the manuscript.

Comment C 1.15 — Tab. 3: Add explanation for numbers in brackets. Is this 1-sigma uncertainty?

Reply: The number in parenthesis are the percentage number. We have added to the caption of Table 3: "The table shows [...] (in ppb and in percentages between parenthesis)."

Comment C 1.16 — Typo in CH4 in several places.

Reply: Thank you for spotting this. Changed CH4 to CH_4

References

Barré, J., Aben, I., Agustí-Panareda, A., Balsamo, G., Bousserez, N., Dueben, P., Engelen, R., Inness, A., Lorente, A., McNorton, J., Peuch, V.-H., Radnoti, G., and Ribas, R.: Systematic detection of local CH4 emissions anomalies combining satellite measurements and high-resolution forecasts, Atmos. Chem. Phys. Discuss., https://doi.org/10.5194/acp-2020-550, in review, 2020.

Response to the reviewers on the manuscript "Methane retrieved from TROPOMI: improvement of the data product and validation of the first two years of measurements" by Alba Lorente et al.

The authors would like to thank the reviewers for their thoughtful and helpful comments and suggestions. Below are the comments by the reviewers in blue and replies in black. Any modification made to the text has been underlined. The line and page numbers correspond to the version of the manuscript available for online discussion.

Reviewer 2

Comment C 2.1 — Page 4, line 5. How do you determine the position of the 12 pressure layers? Are they fixed for every scene or are they calculated with respect to the surface pressure or tropopause height? If the location of the tropopause isn't accounted for in the construction of vertical layers, have you considered the uncertainty this could cause in calculating the total column XCH_4, compared to a method which aims to put a pressure layer boundary at the tropopause height?

Reply: The equidistant pressure layers are determined by the surface pressure and the top of atmosphere from the meteorological input, constrained by a value of 0.1 hPa. So the grid differs per retrieval, and during a single retrieval it remains fixed as the algorithm does not retrieve surface pressure. For the a priori vertical profile we use TM5 that varies with latitude, longitude and altitude also accounting for the effect of tropopause height variations.

Comment C 2.2 — Page 4, line 12. Could you please be more specific in which ECMWF data you are using. Is it ERA-5 or ERA-Interim for example.

Reply: The ECMWF data that we use is an operational analysis product; it corresponds to the first analysis performed after the forecast product, so it is not a reanalysis product as ERA-5 or ERA-Interim. Access to this ECMWF product is granted to us on behalf of the TROPOMI project. We have added "operational analysis product" to the text to make it clearer.

Comment C 2.3 — Page 4, line 21. How well do the results of the back-up filter compare to the VIIRS cloud filter data when you try to use it for scenes where you do have VIIRS to validate it? How many scenes in total for your two years of data use the VIIRS cloud clearing method, and how many use the back-up H2O retrieval method?

Reply: The cloud filtering is important in our processing, so we acknowledge the referee bringing it up, and we hope to clarify it as the Referee #1 also raised a question on this topic.

The quality of our XCH_4 retrieval relies on a very strict cloud filtering, for which we use VIIRS data that is able to identify small-scale cloud structures that could lead to errors in the retrieval if not filtered properly. VIIRS data used in the TROPOMI XCH_4 retrieval is processed operationally by the S5P-NPP cloud processor. If due to any circumstance the processing of the VIIRS data fails or it is delayed, we use the filtering based on a non-scattering retrieval as a back-up option. In this circumstance, the XCH_4 data is flagged (qa value downgraded to 0.4) as the data might be affected by cloud contamination, because the non-scattering retrieval is not as effective filter as VIIRS data, particularly for thick clouds. Originally, the filter based on the the non-scattering retrieval was optimized to filter cirrus over dark surfaces (Hasekamp et al., 2019), by applying a 6% and 22% threshold for the difference between the CH_4 and H_2O retrieved in the weak and strong absorption bands. This filter alone will effectively remove scenes with a cloud fraction higher than 15%, a fraction that is too high to keep the errors in the retrieved CH_4 below requirements. Together with the scattering filter (using the retrieved scattering parameters) scenes with a cloud fraction higher than 8% will be effectively filtered, but still far from the desired 1-2% for the CH_4 retrieval (Hasekamp et al., 2019). These numbers presented here correspond to the analysis made prior to launch, that need to be repeated using real data.

As VIIRS data is operationally processed, it is rarely missing or not available for its use in the XCH_4 retrieval. From all the orbits processed operationally since the beginning of the mission, for less than 1% the processing of VIIRS data was not nominal in the CH_4 retrieval. We added the following to stress this point: "In less than 1% of the cases when VIIRS data is not available, we use a back-up filter based on a non-scattering H_2O and CH_4 retrieval from the weak and strong absorption bands (Hu et al., 2016). These cases are flagged accordingly by the quality value indicator."

Comment C 2.4 — Page 4, lines 24-26. I am a little confused by how you cite a paper from 2019 (Hasekamp et al. 2019) to say that results of version 1.2.0 from June 2020 of your algorithm largely comply with mission requirements. Please could you elaborate on this.

Reply:

Hasekamp et al. (2019) is the reference to the ATBD for the operational algorithm version 1.2.0 mentioned in that sentence. We agree with the reviewer that this might be confusing for the reader, so we remove "as of June 2020". We wanted to specify the version of the operational algorithm when the manuscript was written/submitted (and that is why we added "as of June 2020"), having in mind that this version could have changed in the meantime. But we acknowledge that with the version number it should be sufficient to trace it back.

Comment C 2.5 — Page 4, line 27. You call this new version the beta version here, but do not refer to this again. However, on page 6, line 20 you say the updates to the algorithm correspond

to v1.3.0. Is there a difference between this beta version and 1.3.0? If not then it might be clearer to call it v 1.3.0 here on page 4.

Reply: We acknowledge that the naming and version numbers might led to confusion when reading it, a remark also made by Referee #1 in comment C1.6. We try to make it clearer through the manuscript.

The reference to *beta version of the TROPOMI XCH_4 data product* is used for the data product that results from the scientific development activities within the L2 team at SRON. The next step for these developments is to be implemented in the operational processing whenever there is a a processor update.

We have removed the reference to version 1.3.0 that will eventually correspond to the future operational update, because this specific numbering is not certain as of now, and only causes confusion. Now page 6, line 20 reads: "The TROPOMI XCH_4 scientific data product from SRON retrieved with the updated algorithm will be suggested for use in the operational processing in the next processor update."

Comment C 2.6 — Page 5, line 8. Could you please comment on why you chose to use daily averaged TCCON instead of averaging only data which is within a shorter time frame. I understand that TROPOMI has 14 orbits in one day so I would assume it likely that more than one orbit may intersect the 600km diameter co-location criteria. Do you think there is merit in being stricter in your temporal co-location as a result so you are only matching TCCON at a similar time to an overpass?

Reply: We are glad that this was brought up as we do limit the TCCON measurements to $\pm$ 2 hours of the TROPOMI overpass, so the explanation on the manuscript is wrong, and we have changed it accordingly.

The mistake on the text is because we performed sensitivity tests by also using daily averages. Figure R1 shows the validation results with time constraint (left, same as Fig. 8a in the original manuscript) and without any time constraint (right). The overall validation results do not change significantly. The mean bias does not change significantly, and the station to station variability is only affected by 1 ppb. The number of collocation pairs did increase significantly (from 3203 to 8351). As an example for the validation over one of the stations, Fig. R2 shows the time series of the bias with time constraint (left) and without any time constraint (right).

Comment C 2.7 — Page 6, line 4. I think it's potentially misleading to say that the GOSAT swath is 790km with a 10.5km resolution without saying that its measurement method is different to TROPOMI's and that it usually only makes 3 of those 10.5km measurements across its swath. I think an additional sentence here on the sampling pattern of GOSAT would be helpful.

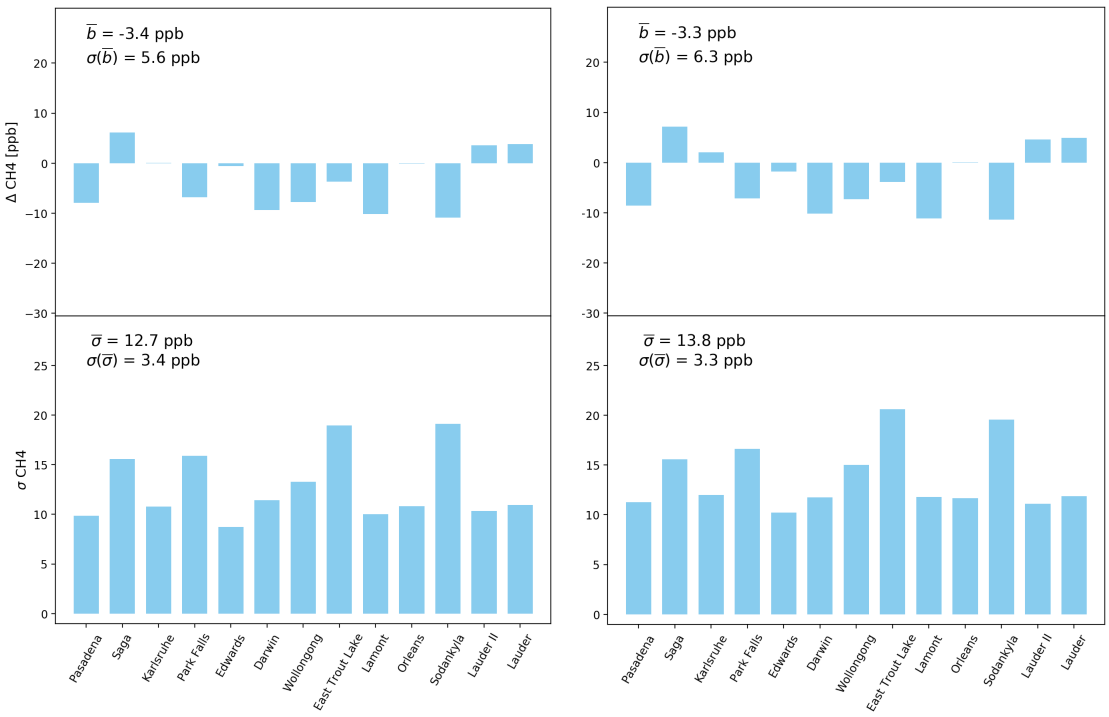

Figure R1: Mean differences between TROPOMI and TCCON XCH_4 (ΔXCH_4) and the standard deviation of the differences (σ_{XCH_4}) with (left) $\pm$ 2 hours of time constraint in TCCON (as in the manuscript) and (right) daily averages.

Reply: We have modified the sentence in page 6, line 4: "GOSAT was launched in 2009, and ~~with a~~ it performs three point observations in a cross-track swath of 790 km with 10.5 km resolution on the ground at nadir, which results in global coverage ~~is obtained~~ approximately every 3 days".

Comment C 2.8 — Page 6, line 16. You use a full-physics method for TROPOMI because the proxy method cannot be applied, and go on to say that the full-physics and proxy methods were found to perform similarly for GOSAT. What you don't explain in the paper is why you don't use the GOSAT full-physics data as this feels like a more natural comparison. Could you please comment on why you used gosat proxy over gosat full-physics?

Reply: The main reason to use the proxy product in this comparison is the fact that the data yield is higher. Furthermore, the comparison of TROPOMI XCH_4 and GOSAT with both approaches results in similar bias: mean bias of -10.3 ± 16.8 ppb and a Pearson's correlation coefficient of 0.85 with the proxy approach (as stated in the manuscript) and mean bias of -12.5 ± 14.9 ppb and

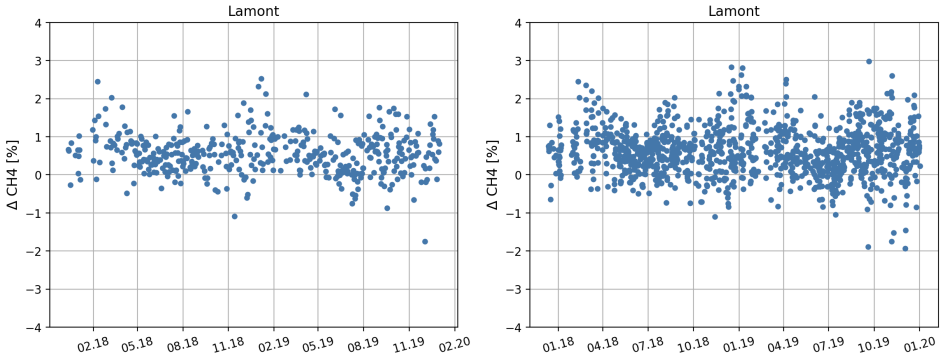

Figure R2: Time series of the bias between TROPOMI and TCCON XCH_4 over the Lamont station with time constraint (left) and without time constraint (right).

a Pearson's correlation coefficient of 0.86 with the full physics approach. The correlation plot of both comparisons is shown in Fig. R3, on the left for GOSAT proxy and on the right for GOSAT full-physics.

We have added this information to make clear the reason for the selection of the full-physics approach (page 6, line 15): "In the validation in Sect. 5 we found that there is no bias between the GOSAT proxy and full-physics products. However, we have selected for the comparison the GOSAT proxy product over the full-physics because of its higher data yield". And we also include the results for the full-physics in a sentence in page 17, line 7: "The overall comparison yields a mean bias of -12.5 ± 14.9 ppb if we use the GOSAT XCH_4 product retrieved with the full-physics approach".

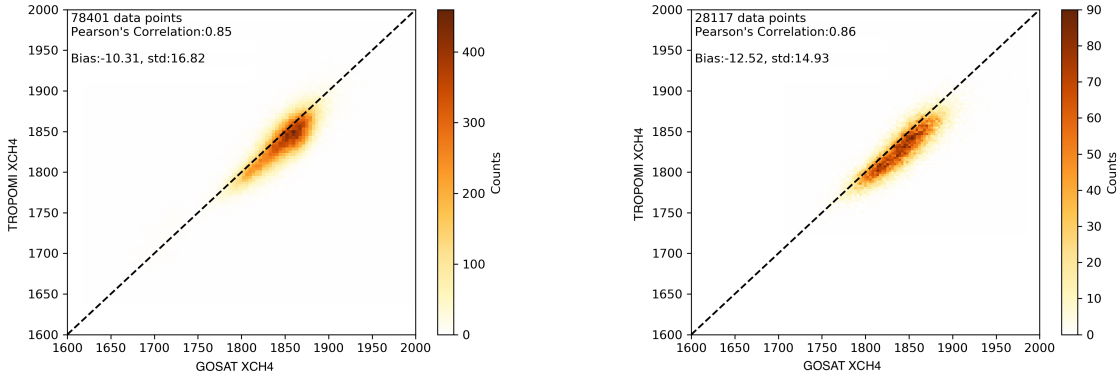

Figure R3: Correlation plot of TROPOMI XCH_4 and GOSAT XCH_4 retrieved with the proxy approach (left) and with the full physics (right). Daily collocations are averaged to a 2°x2° grid for the period 1 Jan 2018 – 31 Dec 2019.

Comment C 2.9 — On Section 3.1. It makes sense to me that using a constant gamma reduces the overall dispersion of the data, improving your results. But please can you comment on the theory behind why you think calculating gamma per iteration should result in a less accurate result than using an average value.

Reply: In theory calculating a gamma for each iteration should be actually superior than using an average gamma value. However, it is based on the idea of finding the minimum value of the elbow plots (χ^2 vs. regularization strength). Using real data, such a minimum does not exist in most cases and therefore can result in a more unstable inversion. We found using an average value for gamma results in a more stable retrieval and reduces the overall dispersion of the data.

Comment C 2.10 — Page 7, line 12. The reduction of 9% going from 19.7 ppb to 24.5 ppb doesn't make sense to me since it's becoming larger instead of reducing and the difference between these numbers is larger than 9%.

Reply: We appreciate the careful reading of the referee that led to spotting this typo. The reduction is from 21.5 ppb (and not 24.5) to 19.7 ppb, which corresponds to approximately 9%. We have corrected this.

Comment C 2.11 — Page 7, line 25. In your section on the TCCON validation you say that the overall bias with respect to HITRAN 2008 is +15.5 for HITRAN 2016. Table 2 shows that the difference between HITRAN 2008 and HITRAN 2016 is 20.3 ppb for TCCON.

Reply: We thank again for this careful check of the numbers. Indeed the bias from -2.4 ppb to 17.9 ppb is 20.3 and not 15.5 as it is written in the text (this is considering HITRAN 2008 bias as 2.4 ppb and not -2.4 ppb). We have corrected the text accordingly.

Comment C 2.12 — Page 7, line 31. Please could you give the global numbers as referred to here which show that SEOM-IAS has a significantly improved RMS and chi-squared over the other two.

Reply: We added these numbers to the text, page 7, line 31. "Global mean χ^2 improves by 19% with SEOM-IAS cross-section and by 7% with HITRAN 2016 with respect to HITRAN 2008".

Figure R4 shows the ratio of χ^2 of the retrieval with HITRAN 2008 and HITRAN 2016 (left) and HITRAN 2008 and SEOM-IAS (right), for one year of data averaged into daily 1° x 1° grid, which shows that SEOM-IAS cross section results in a significantly better χ^2 with respect to HITRAN 2008 and HITRAN 2016.

Comment C 2.13 — On section 3.3. I like the discussion on the differences of greater than 45m and 50m, but in figure 2 there are a lot of smaller systematic differences of 10-20m to be seen in

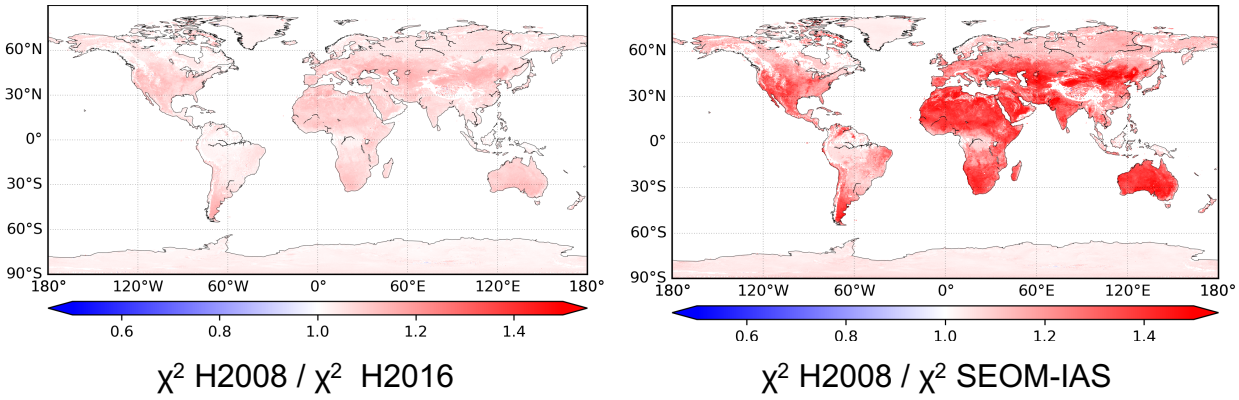

Figure R4: Ratio of χ^2 from the retrieval with HITRAN 2008 and HITRAN 2016 (left) and SEOM-IAS (right).

the Eastern US which lead to a net positive XCH4 difference over this half of the country. Firstly, please could you comment on why you think the higher resolution DEM would be on average higher elevation than the lower-res DEM over this region. And following on, could you please comment on the change to XCH4 overall as a result of any mean altitude difference between DEMs on a global scale (if one exists). I ask since you only focus on outliers between the DEMs in the paper and don't talk about any systematic differences.

Reply: The different East-West features over United States shown in Fig. 2 are only present in this region. As why on average the SRTM results higher in elevation over Eastern US we are not sure, but we assume that compared to the S5P-DEM, the SRTM database is a better representation on the terrain over the US as it is a database that uses national data and models. Globally, we see similar features as in the Western US in most of the mountain regions around the world, so there are not systematic differences. So overall XCH_4 changes are more pronounced over mountain regions, that is why we focused on the outliers in the discussion on Sect. 3.3.

Comment C 2.14 — On the Small Area Analysis. Could you please elaborate on how and why you chose the areas which you did. How dependent on your method is the choice of SAAs.

Reply: The reasoning for the choice of the specific areas used in the SAA analysis was mainly to have a representation of the challenging scenes for the XCH_4 retrieval, mainly low and high albedo. The areas also needed to include scenes with surface albedo around the reference value, and not include (as much as possible) big sources of methane, although this was less of a limiting factor because XCH_4 distribution is normalized for each region separately. Furthermore, we aimed at areas that had a relatively good coverage through all the different seasons, and we stayed away from big mountain regions.

For high albedo scenes it was straightforward to chose Sahara desert, and over this area we

tested the choice of multiple regions and their size. The main challenge was to find regions that included the surface albedo reference value, and all the areas that we tested resulted in similar XCH_4 dependencies. Over Australia we made boxes of 5°x 5° and discarded those that had in the same box different modes in the XCH_4 distribution with respect to surface albedo. The most southern box was interesting because it includes low surface albedo values with strong XCH_4 underestimation, and the shape of this area is different to 5°x5° to avoid the location of strong XCH_4 sources as present in the EDGAR inventory (it is a region with an important oil and gas industry). Then areas over Canada were chosen because it represents the strong XCH_4 underestimation related to the low surface albedo values in these high latitudes, also present in Northern part of Europe and Russia. Adding areas of Russia did not change the dependence and the fit (Fig. 4) made to derive the correction.

Comment C 2.15 — On the bias correction method, page 10, line 1. You only apply a bias correction on the surface albedo and say that the other retrieved parameters show negligible dependence, showing surface albedo, AOD and SZA. For OCO-2 the parameter dP (the difference between the a priori and retrieved surface pressure) shows the largest dependence on the bias. Is this a parameter you have looked in to?

Reply:

In the TROPOMI XCH_4 retrieval we do not retrieve surface pressure. In Fig. 3 in the manuscript we show surface albedo, AOD and SZA as an example, but dependencies in other parameters such as χ^2, column of interfering absorbers H_2O and CO, retrieved aerosol parameters (aerosol size, altitude of aerosol distribution and aerosol column) were also investigated. Besides the fact that we also tried to use as few correction parameters as possible, all the other parameters showed negligible dependence compared to that on surface albedo. We have specified that SZA and AOD are examples on page 10, line 3 to avoid misunderstanding.

Comment C 2.16 — Page 16. Lines 5-6. Have you tried comparing with snow cover data to verify how reliable this method of detecting snow actually is?

Reply: We have not done that comparison ourselves, but we are in contact with colleagues from the Finish Meteorological Institute (FMI) to investigate the seasonality on the bias further. They have found a significant correlation between the seasonality of the bias and the presence of snow surface at Sodankylä, and as the blended albedo is as well correlated to this seasonality, it is suitable to use it to filter this complex scenes, but it is not aimed as an accurate method to actually detect snow. We specify this on page 17, line 1: "By applying it [...] a threshold value of 0.85 is optimal to remove these scenes that cause the seasonality on the bias". However, we do not apply this filter ourselves in an operational mode, as the source of these seasonality of the TROPOMI-TCCON bias is still unknown.

The correlation with snow surface found by FMI does not necessarily always imply the presence of vortex air which was our first hypothesis to explain the seasonality of the bias. We are also investigating the role of the prior profile in this specific retrieval scenarios, assuming that there might be cases with a strong depletion of XCH_4 in the upper troposphere (due mainly to vortex air) that impact our retrieval (and/or TCCON) if it is not captured properly by the prior. Furthermore, the different sensitivities between TCCON and TROPOMI might also play a role in the satellite and ground based comparison. All these effects we think need to be taken into account when making conclusions out of the validation results.

Comment C 2.17 — Page 5, Table 1. Caption missing versions for the instrument.

Reply: We assume that this refers to the typo as both instruments are referred as "ll" in the caption of Table 1. The instrument "ll" (Sherlock et al., 2017) was replaced by "lr" (Pollard et al., 2019). We have corrected this.

Comment C 2.18 — Page 10, line 7. Typo with full stop. I assume you wanted a capital T or a semicolon.

Reply: Corrected.

Comment C 2.19 — There are multiple instances throughout the paper where you've misspelt ppb as pbb. Such as Page 7 line 25, page 9 line 8, page 20 line 16 and twice on page 14 line 4.

Reply: We thank the referee for spotting this. We have changed it.

Methane retrieved from TROPOMI: improvement of the data product and validation of the first two years of measurements

Alba Lorente[1], Tobias Borsdorff[1], Andre Butz[2,3], Otto Hasekamp[1], Joost aan de Brugh[1], Andreas Schneider[1], Lianghai Wu[1], Frank Hase[4], Rigel Kivi[5], Debra Wunch[6], David F. Pollard[7], Kei Shiomi[8], Nicholas M. Deutscher[9], Voltaire A. Velazco[9], Coleen M. Roehl[10], Paul O. Wennberg[10], Thorsten Warneke[11], and Jochen Landgraf[1]

[1]Earth science group, SRON Netherlands Institute for Space Research, Utrecht, the Netherlands
[2]Institute of Environmental Physics, University of Heidelberg, Heidelberg, Germany
[3]Heidelberg Center for the Environment, University of Heidelberg, Heidelberg, Germany
[4]Institute of Meteorology and Climate Research (IMK-ASF), Karlsruhe Institute of Technology, Karlsruhe, Germany
[5]Greenhouse Gases and Satellite Methods group, Finnish Meteorological Institute, Sodankylä. Finland
[6]Department of Physics, University of Toronto, Toronto, Canada
[7]National Institute of Water and Atmospheric Research Ltd (NIWA), Lauder, New Zealand
[8]Japan Aerospace Exploration Agency (JAXA), Tsukuba, Japan
[11]Institute of Environmental Physics, University of Bremen, Bremen, Germany
[9]Centre for Atmospheric Chemistry, School of Earth, Atmospheric and Life Sciences, University of Wollongong, Wollongong, NSW, 2522
[10]Division of Geological and Planetary Sciences, California Institute of Technology, Pasadena, California, USA

Correspondence: Alba Lorente (a.lorente.delgado@sron.nl)

Abstract. The TROPOspheric Monitoring Instrument (TROPOMI) aboard of the Sentinel 5 Precursor (S5-P) satellite provides methane (CH_4) measurements with high accuracy and exceptional temporal and spatial resolution and sampling. TROPOMI CH_4 measurements are highly valuable to constrain emissions inventories and for trend analysis, with strict requirements on the data quality. This study describes the improvements that we have implemented to retrieve CH_4 from TROPOMI using the RemoTeC full-physics algorithm. The updated ~~TROPOMI CH_4 product~~ retrieval algorithm features a constant regularization scheme of the inversion that stabilizes the retrieval and yields less scatter in the data, and includes a higher resolution surface altitude database. We have tested the impact of three state-of-the-art molecular spectroscopic databases (HITRAN 2008, HITRAN 2016 and Scientific Exploitation of Operational Missions – Improved Atmospheric Spectroscopy Databases SEOM-IAS) and found that SEOM-IAS provides the best fitting results. The most relevant update in the TROPOMI XCH_4 data product is the implementation of a posteriori correction fully independent of any reference data that is more accurate and corrects for the underestimation at low surface albedo scenes and the overestimation at high surface albedo scenes. After applying the correction, the albedo dependence is removed to a large extent in the TROPOMI versus satellite (Greenhouse gases Observing SATellite – GOSAT) and TROPOMI versus ground-based observations (Total Carbon Column Observing Network – TCCON) comparison, which is an independent verification of the correction scheme. We validate two years of TROPOMI CH_4 data that shows the good agreement of the updated TROPOMI CH_4 with TCCON (-3.4 ± 5.6 ppb) and GOSAT (-10.3 ± 16.8 ~~pbb~~ppb) (mean bias and standard deviation). Low and high albedo scenes as well as snow covered scenes are the most

challenging for the CH_4 retrieval algorithm, and although the posteriori correction accounts for most of the bias, there is a need to further investigate the underlying cause.

1 Introduction

Methane (CH_4) is the second most important anthropogenic greenhouse gas after carbon dioxide (CO_2). The global warming potential of CH_4 for a 20 year horizon is more than 80 times higher than that of CO_2 (Myhre et al., 2013), and together with its relatively short lifetime of about 10 years makes it an ideal short-term target for climate change mitigation strategies via reducing CH_4 emissions. CH_4 has both natural (e.g. wetlands) and anthropogenic sources (e.g. agriculture and waste together with fossil fuels), and globally 60 % of the total emissions are attributed to anthropogenic sources (Saunois et al., 2019). Natural sources are the most uncertain components of the CH_4 budget because of their magnitude and variability, which at the same time depend on characteristics that are vulnerable to changes in the state of the Earth's climate. Furthermore, the interpretation of observed CH_4 trends is hampered by the uncertainties in the estimates of CH_4 emissions (Turner et al., 2019).

Satellite observations of CH_4 are highly valuable to constrain emission inventories and for trend analysis, not only at global scale but also at regional and local scales. CH_4 measurements from satellite instruments like GOSAT (Greenhouse gases Observing SATellite) have been used to infer CH_4 emissions from natural sources (e.g. tropical wetlands (Lunt et al., 2019)) and anthropogenic sources (e.g. coal mining in China (Miller et al., 2019)), and also to map emissions and trends at global scale (e.g. Maasakkers et al. (2019)). However, the spatial and temporal resolution at which these emissions can be resolved is limited by the capabilities of the instrument, preventing daily estimations or source attribution at fine scales.

A unique perspective for the long-term monitoring of CH_4 is provided by the TROPOMI (TROPOspheric Monitoring Instrument) instrument on board the Sentinel 5 Precursor (S5-P) satellite with its daily global coverage at an unprecedented resolution of 7×7 km^2 since its launch in October 2017 (upgraded to 5.5×7 km^2 in August 2019). The high resolution together with the high signal-to-noise ratio allows the detection and quantification of CH_4 emissions from localized (e.g. Pandey et al. (2019)) to larger scale sources (e.g. Permian basin by ~~Zhang et al. (2020)~~Schneising et al. (2020); Zhang et al. (2020)). Furthermore, assimilating TROPOMI CH_4 has shown great potential (e.g. in the Copernicus Atmosphere Monitoring Service (CAMS) ECMWF Integrated Forecasting System (CAMS-IFS) data assimilation system ~~(Barre et al. , 2020)).~~ (Barré et al., 2020). The main challenge of CH_4 remote sensing is that high data quality is required for data assimilation and flux inversion applications. For TROPOMI, strict mission requirements are formulated with a single sounding precision and accuracy both below 1% (Veefkind et al., 2012).

TROPOMI CH_4 operational data was already proved to be of good quality by comparisons shortly after launch with both GOSAT observations (Hu et al., 2018) and ground-based measurements from the TCCON network (Hasekamp et al., 2019). However, the CH_4 data product can be now further improved using real measurements after TROPOMI has been measuring for more than two years. A detailed analysis of the data provides insight on which aspects of the processing chain regarding the input data or retrieval algorithm can be further improved. The long-term record also allows to explore possibilities of correcting biases independent of any reference data (e.g. ground-based or other satellite measurements).

In this study we present the improvements that we have developed to retrieve CH_4 from TROPOMI measurements using the full-physics approach, and we validate the TROPOMI CH_4 product with satellite and ground-based measurements. Section 2 describes the data and analysis methods that we use and Sect. 3 focuses on the main improvements related to the regularization scheme of the inversion, the choice of the spectroscopic database for the absorption cross sections, the surface elevation database and a posteriori bias correction derived using only TROPOMI data. Finally, Sect. 4 and Sect. 5 show a detailed validation of the improved TROPOMI CH_4 data. The study concludes in Sect. 6 with an outlook for future steps regarding CH_4 data retrieved from TROPOMI.

2 Retrieval algorithm and validation data sets

2.1 TROPOMI CH_4 retrieval algorithm

The methane total column-average dry-air mole fraction (XCH_4) is retrieved from TROPOMI measurements of sunlight backscattered by Earth's surface and atmosphere in the near-infrared (NIR) and shortwave-infrared (SWIR) spectral bands with the retrieval algorithm RemoTeC. This algorithm has been extensively used to retrieve both CO_2 and CH_4 from measurements of OCO-2 and GOSAT (e.g. Wu et al. (2018); Butz et al. (2011)) and it is the Sentinel 5-P and Sentinel 5 operational algorithm for CH_4 (Hasekamp et al. (2019); Landgraf et al. (2019)).

The S5P RemoTeC algorithm uses the full-physics approach that simultaneously retrieves the amount of atmospheric CH_4 and the physical scattering properties of the atmosphere. The algorithm aims at inferring the state vector $\boldsymbol{x}$ that contains all the parameters to be retrieved from the radiance measurements $\boldsymbol{y}$ in the SWIR (2305-2385 nm) and NIR (757-774 nm) spectral bands, where the forward model $\boldsymbol{F}$ simulates the TROPOMI measurements,

$$\boldsymbol{y} = \boldsymbol{F}(\boldsymbol{x}) + \epsilon_y + \epsilon_F. \tag{1}$$

Here, ϵ_y and ϵ_F are the measurement noise error and the forward model error respectively. The forward model employs the LINTRAN V2.0 radiative transfer model in its scalar approximation to simulate atmospheric light scattering and absorption in a plane parallel atmosphere (Schepers et al. (2014); Landgraf et al. (2001)). Accurate modelling of absorption by molecules relies on spectroscopic databases, which provide the absorption cross-section of the target absorber CH_4 as well as of the interfering gases CO, H_2O and O_2.

The inversion to estimate the state vector $\boldsymbol{x}$ requires the use of regularization methods, as measurements typically do not contain sufficient information to retrieve every state vector element independently. The RemoTeC retrieval algorithm uses the Philips-Tikhonov regularization scheme, which aims to find the state vector by solving the minimization problem

$$\hat{\boldsymbol{x}} = \min\Big(||\boldsymbol{S}_y^{-1/2}(\boldsymbol{F}(x) - \boldsymbol{y})||^2 + \gamma||\boldsymbol{W}(\boldsymbol{x} - \boldsymbol{x}_a)||^2\Big), \tag{2}$$

where $||\cdot||$ describes the Euclidian norm, $\boldsymbol{S}_y$ is the measurement error covariance matrix that contains the noise estimate, γ is the regularization parameter, $\boldsymbol{W}$ is a diagonal weighting matrix that renders the side constraint dimensionless and ensures that only the target absorber CH_4 and the scattering parameters contribute to its norm (Hu et al., 2016), and $\boldsymbol{x}_a$ is the a priori state vector.

The retrieval state vector contains CH_4 partial sub-column number densities at 12 equidistant pressure layers. The total column of the interfering non-target absorbers CO and H_2O are also retrieved, together with the effective aerosol total column, size and height parameter of the aerosol power law distribution. A Lambertian surface albedo in both NIR and SWIR spectral range together with its first order spectral dependence is also retrieved, as well as spectral shift and fluorescence in the NIR band.

The TROPOMI CH_4 data product is given in the form of total column-averaged dry-air mole fraction, XCH_4. It is calculated from the methane vertical subcolumn elements x_i and the dry air column $V_{\mathrm{air,dry}}$ calculated with meteorology input from ECMWF (European Centre for Medium-Range Weather Forecasts) operational analysis product and surface topography from a high resolution database:

$$\mathrm{XCH_4} = \sum_{i=0}^{n} \frac{x_i}{V_{\mathrm{air,dry}}}. \tag{3}$$

The precision $\sigma_{\mathrm{XCH_4}}$ ~~is given~~ available in the data product is defined as the standard deviation of the retrieval noise, which follows from the error covariance matrix $\boldsymbol{S}_x$ that describes the effect of the measurement noise on the retrieval (Hu et al., 2016):

$$\sigma_{\mathrm{XCH_4}} = \frac{\sqrt{\sum_{i,j=0}^{n} S_{x,i,j}}}{V_{\mathrm{air,dry}}} \tag{4}$$

The algorithm has been designed to provide accurate and precise retrievals for clear-sky scenes with minor scattering by aerosols and optically thin cirrus. To fulfill this criterion, a strict cloud filter is applied based on observations of the Visible Infrared Imaging Radiometer Suite (VIIRS) aboard the Suomi-NPP satellite that observes the same scene as TROPOMI approximately 5 minutes earlier. In less than 1% of the cases when VIIRS data is not available, we use a back-up filter based on a non-scattering H_2O and CH_4 retrieval from the weak and strong absorption bands (Hu et al., 2016). These cases are flagged accordingly by the quality value indicator. Table A1 summarizes the filters applied in the retrieval process and in the TROPOMI data selection used in this study.

The CH_4 total column-average dry-air mole fraction retrieved from TROPOMI with the operational retrieval algorithm (version 1.2.0~~as of June 2020~~) largely complies with the mission requirement of precision and accuracy below 1%, with significantly improved data quality of the bias-corrected product (Hasekamp et al., 2019). In Sect. 3 we present recent updates that further improve the quality of the data. ~~This updated retrieval algorithm is referred to as the beta-version of the TROPOMI XCH~~The TROPOMI XCH_4 ~~data product.~~ scientific data product from SRON retrieved with the updated algorithm serves as a beta version of the operational processing. Another scientific retrieval algorithm using the Weighting Function Modified

Differential Optical Absorption Spectroscopy (WFM-DOAS) method to retrieve CO and CH_4 from TROPOMI was presented by Schneising et al. (2019). Comparison of both retrieval approaches is foreseen as part of ongoing verification activities.

2.2 TCCON reference dataset

To validate XCH_4 retrieved from TROPOMI we use independent ground-based XCH_4 measurements from the Total Carbon Column Observing Network (TCCON) (Wunch et al., 2011a) as a reference (data version GGG2014). Table 1 contains the information of the 13 different stations located in North America, East Asia, Europe and Oceania used for the validation. In regions where there are multiple TCCON stations, we have selected those located at flat terrain in relatively remote areas, which minimizes the errors due to assumptions on the vertical CH_4 distribution used to correct for differences between the surface elevation of TROPOMI particular pixels and the ground altitude at the TCCON sites.

Table 1. Overview of the stations from the TCCON network used in this study.

Site (Country)	Coordinates Lat, Lon (°)	Altitude (m.a.s.l.)	Reference
Sodankylä (Finland)	67.37, 26.63	190	Kivi and Heikkinen (2016) Kivi et al. (2017)
East Trout Lake (Canada)	54.36, -104.99	500	Wunch et al. (2017)
Karlsruhe (Germany)	49.1, 8.44	110	Hase et al. (2017)
Orléans (France)	47.97, 2.11	130	Warneke et al. (2017)
Park Falls (US)	45.94, -90.27	440	Wennberg et al. (2017a)
Lamont (US)	36.6, -97.49	320	Wennberg et al. (2017b)
Pasadena (US)	34.14, -118.13	240	Wennberg et al. (2017c)
Edwards (US)	34.95, -117.88	30	Iraci et al. (2016)
Saga (Japan)	33.24, 130.29	10	Kawakami et al. (2017)
Darwin (Australia)	-12.46, 130.93	30	Griffith et al. (2017a)
Wollongong (Australia)	-34.41, 150.88	30	Griffith et al. (2017b)
Lauder* (New Zealand)	-45.04, 169.68	370	Sherlock et al. (2017) Pollard et al. (2019)

*For the Lauder station the *ll* instrument was replaced on October 2018 by the *lr* instrument.

To evaluate the quality of the retrieved TROPOMI XCH_4, we average TROPOMI XCH_4 data within a collocation radius around each station of 300 km. The average retrieved TROPOMI XCH_4 within the specific radius is compared with ~~daily average~~ measurements of the matching TCCON station ~~(i.e. no time constraint)~~ (within ± 2 hours of the TROPOMI overpass ($XCH_{4,\mathrm{TROPOMI}} - XCH_{4,\mathrm{TCCON}}$). For all paired collocations at each station, we compute the mean bias defined as the mean of the difference of individual collocations (ΔCH_4) and its standard deviation (σ) as a measure of the spread in the data. We then compute the average of the station biases ($\bar{b}$) and its standard deviation ($\sigma(\bar{b})$) as a measure of the station-to-station

variability. The station-to-station variability is an important diagnostic parameter as it indicates regional biases in our data, and it might be used as an overall uncertainty estimate.

2.3 GOSAT reference dataset

XCH_4 measurements by The Thermal And Near infrared Sensor for carbon Observation - Fourier Transform Spectrometer (TANSO-FTS) on board the Greenhouse gases Observing SATellite (GOSAT) satellite are used for the validation of the TROPOMI XCH_4 data. GOSAT was launched in 2009, and ~~with a~~ it performs three point observations in a cross-track swath of 790 km ~~and~~ with 10.5 km resolution ~~, global coverage is obtained~~ on the ground at nadir, which results in global coverage approximately every 3 days.

We use the GOSAT proxy XCH_4 data product produced at SRON in the context of the ESA GreenHouse Gas Climate Change Initiative (GHG CCI) project (Buchwitz et al., 2019, 2017). This XCH_4 product is retrieved using the RemoTeC/proxy retrieval algorithm. The proxy approach (Frankenberg et al., 2005) infers a CO_2 and CH_4 total column from observations at 1.6 µm ignoring any atmospheric scattering in the retrieval. Substantially, the XCH_4 product is derived by

$$\mathrm{XCH_4}^{\mathrm{proxy}} = \frac{V_{\mathrm{CH_4}}}{V_{\mathrm{CO_2}}} \cdot \mathrm{XCO_2}^{\mathrm{mod}} \tag{5}$$

where the column-average dry-air mole fraction $\mathrm{XCO_2}^{\mathrm{mod}}$ is taken from the Carbon Tracker data assimilation system, and V_{CH_4} and V_{CO_2} are the vertical column densities. This approach assumes that light path modifications due to scattering in the atmosphere are the same for the target absorber (i.e. CH_4) and the proxy absorber CO_2, whose prior is assumed to be known with high accuracy.

In the validation in Sect. 5 we found that there is no bias between the GOSAT proxy and full-physics products. However, we have selected for the comparison the GOSAT proxy product over the full-physics because of its higher data yield. The proxy approach cannot be applied to retrieve XCH_4 from TROPOMI since it does not cover the 1.6 µm CH_4 and CO_2 absorption bands. Schepers et al. (2012) compared both the physics and proxy retrievals applied to GOSAT measurements to retrieve XCH_4 and concluded that both retrievals performed similarly with respect to bias variability and precision when validating the retrieved XCH_4 with ground-based TCCON measurements. This study also concluded that both methods can retrieve XCH_4 in aerosol loaded scenes with retrieval errors of less than 1%.

3 TROPOMI CH_4 retrieval updates

~~Our updated~~ The TROPOMI XCH_4 ~~product corresponds to the S5P-RemoTeC algorithm version 1.3.0 that~~ scientific data product from SRON retrieved with the updated algorithm will be suggested for use in the operational processing ~~(Hu et al. (2016) , data product 1.2.0)~~ in the next processor update. The updates to the S5P-RemoTeC retrieval algorithm relate to the regularization scheme, the selection of the spectroscopic database, the implementation of a higher resolution digital elevation map (DEM) for surface altitude and a more sophisticated a posteriori correction for the albedo dependence. In this section we

present the updates and quantify the improvements, and we use the comparison with TCCON and GOSAT as a benchmark to test the performance of the retrieval after implementing the updates.

3.1 Regularization scheme

Hu et al. (2016) determined the regularization parameter γ in the inversion (Eq. 2) using the L-curve criterion (Hansen (1998), Hu et al. (2016)) in each iteration of the TROPOMI measurement inversion. As TROPOMI has been measuring for more than two years, it is possible to select a constant regularization optimized for real observations. This includes a dedicated regularization parameter for the target absorber CH_4 and one for each of the ~~aerosol parameters (~~scattering parameters (effective aerosol distribution height and size parameter, and effective aerosol column). The advantage of the constant regularization is a more stable performance compared to the L-curve method in which the regularization strength changes at each iteration for every scene. The regularization parameters are selected such that the degrees of freedom for CH_4 are between 1 and 1.5 and that retrieved ~~aerosol parameters have realistic distributions~~scattering parameters follow a distribution that we would expect.

The main improvement of the constant regularization is that the dispersion in the retrieved XCH_4 is significantly reduced. This is noticeable in the XCH_4 distribution over small regions where we do not expect large gradients of XCH_4. At regions with relatively low albedo, the decrease in the spread of the data can reach 10-20 % (e.g. from 18 ppb to 14 ppb over Canada and 11 to 9 over Australia). Furthermore, the validation with TCCON shows a decrease in the station-to-station variability of 4 ppb (25 % decrease of the 15 ppb station-to-station variability using the L-curve approach) when analysing one year of data. The comparison with GOSAT shows that the new regularization scheme reduces the standard deviation of the difference between collocated GOSAT and TROPOMI XCH_4 observations by 9 % (~~19.7 ppb to 24.5~~ from 21.5 ppb to 19.7 ppb).

3.2 Spectroscopy database

The TROPOMI CH_4 retrieval uses external spectroscopic information to simulate the molecular absorption lines of the target absorber CH_4 as well as of CO and H_2O. The baseline retrieval algorithm employs the HITRAN 2008 spectroscopic database (Rothman et al., 2009) with updated spectroscopy parameters for H_2O from Scheepmaker et al. (2013). In preparation for the Sentinel 5 Precursor mission, Birk et al. (2017) established an improved spectroscopic database, the so-called "Scientific Exploitation of Operational Missions - Improved Atmospheric Spectroscopy Databases" (SEOM-IAS hereafter) for the interpretation of TROPOMI observations. The release of the HITRAN 2016 database already included some of the updates from the SEOM-IAS project regarding H_2O (Gordon et al., 2017). We have tested the effect of the three spectroscopic databases on the retrieved XCH_4 using one year of TROPOMI data (Sep 2018 - Sep 2019).

The TCCON validation shows that after substituting HITRAN 2008 by HITRAN 2016 and SEOM-IAS for all the molecules in the CH_4 retrieval, the station-to-station variability does not change significantly (less than 1 ppb, see Table 2). The change in the mean bias shows that the different spectroscopy databases introduce an overall bias in the retrieved XCH_4 with respect to HITRAN 2008 (+~~15.5 pbb~~ 20.3 ppb for HITRAN 2016 and -14.7 ppb for SEOM-IAS), but the correlation of the bias with other retrieved parameters (surface albedo, H_2O) does not improve or worsen with any of the spectroscopic database. The spectral fitting quality parameters (e.g. the root mean square of the spectral fit residuals (RMS) and the corresponding χ^2) show

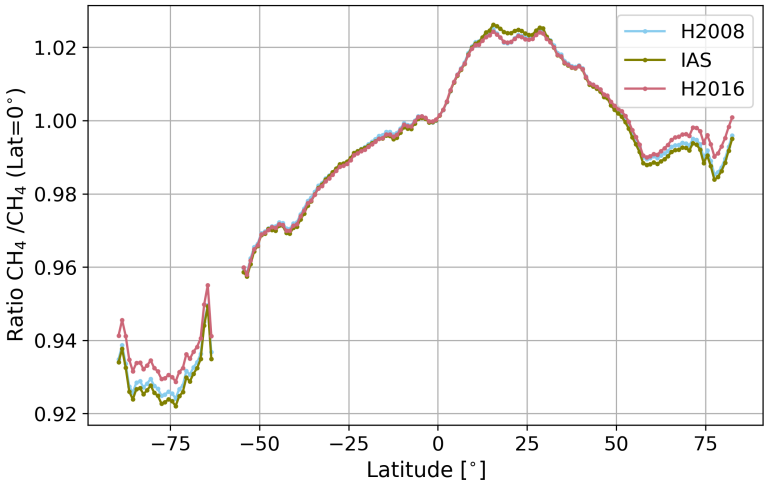

Figure 1. Latitudinal distribution of TROPOMI XCH_4 retrieved using HITRAN 2008 (blue), HITRAN 2016 (pink) and SEOM-IAS (green), referenced to the value at 0° latitude. Daily measurements from Sep 2018 – Sep 2019 are gridded into a 0.2° x 0.2° grid, averaged longitudinally and then binned in 1° latitude.

a slight improvement over TCCON stations when using the SEOM-IAS spectroscopic database, similar to what was found for the CO retrieval from TROPOMI (Borsdorff et al., 2019). The comparison with XCH_4 measured by GOSAT also shows that different spectroscopic database introduce an overall bias but the standard deviation of the bias does not change significantly (Table 2).

On a global scale, we see that both the RMS and χ^2 improve significantly when using the SEOM-IAS database, with HITRAN 2008 giving the worst fitting results. Global mean χ^2 improves by 19% with SEOM-IAS cross-section and by 7% with HITRAN 2016 with respect to HITRAN 2008. Figure 1 shows the latitudinal distribution of XCH_4 retrieved with HITRAN 2008, SEOM-IAS and HITRAN 2016, referenced to the value at 0° latitude. XCH_4 retrieved with HITRAN 2016 shows the least latitudinal variation at latitudes higher than 55° where differences between the datasets are largest, however the global distribution does not point to a better performance of any of the spectroscopic database. The validation with TCCON observations including Eureka (80.05°N) and Lauder (45.04° S) just reflects the overall bias, but does not point to any latitudinal bias of XCH_4 retrieved with any of the spectroscopic database (not shown).

The results of the sensitivity tests do not point to an improved data quality when HITRAN 2016, SEOM-IAS or HITRAN 2008 spectroscopic database is used. Each of them introduces an overall bias that cannot be used as an independent argument to favour a specific database. In view of the better spectral fitting results in the retrieved XCH_4 we have decided to use the SEOM-IAS spectroscopy database.

Table 2. Overview of the TCCON and GOSAT validation results (mean bias and its standard deviation) for the TROPOMI XCH_4 retrieved with different spectroscopic databases.

	$\overline{b} \pm \sigma(\overline{b})$ **CH$_4$[ppb]***
TCCON	
HITRAN 2008	-2.4 ± 11.7
SEOM-IAS	-17.1 ± 12.4
HITRAN 2016	17.9 ± 11.1
GOSAT	
HITRAN 2008	3.9 ± 20.1
SEOM-IAS	-8.4 ± 22.8
HITRAN 2016	23.8 ± 19.7

* b = TROPOMI −ref

3.3 Surface elevation

Satellite remote sensing of XCH_4 requires accurate knowledge of surface pressure and thus of surface elevation, which is specially relevant for the spatially highly resolved measurements of TROPOMI. The effect is two-fold: (1) through the pressure dependence of the absorption cross sections and (2) through the dry air column used to calculate dry air mixing ratio from the retrieved column (Eq. 3).

In a first pre-processing step of the retrieval, the elevation data from a digital elevation map (DEM) is interpolated in space to the ground pixel. Then a correction is applied to the atmospheric variables (i.e. surface pressure and model pressure levels) based on the difference between the coarse resolution ECMWF altitude and the surface elevation from the DEM. To minimize errors, a filter is applied on terrain roughness, which excludes scenes with a standard deviation of the surface elevation higher than 80 m within the observed area. The default source for surface elevation information for all TROPOMI products is the Global multi-resolution terrain elevation data 2010 DEM (GMTED2010) with an aggregation radius of 5 km and a sampling of around 2 km, which results in a resolution of approximately 2 km (S5P-DEM hereafter).

The updated retrieval scheme uses the Shuttle Radar Topography Mission (SRTM) (Farr et al., 2007) digital elevation map with a resolution of 15 arcsec, approximately 400 meters. To match the DEM surface elevation with the ground pixel, we perform a spatial sampling of 0.5 km and compute the mean altitude and its standard deviation for each scene. Figure 2 (upper panel) shows altitude differences between S5P-DEM and SRTM collocated to TROPOMI pixels (before altitude correction) on 5 May 2019 over the United States. In this specific area, 5 % of the pixels have differences in altitude greater than 45 m, with the highest differences over mountain regions. For these scenes the differences in retrieved XCH_4 are up to 7 ~~pbb~~ppb. On a yearly average (and after correction and quality filtering), 1 % of the retrievals present altitude differences greater than 50 m, which result in surface pressure differences above 5 hPa and XCH_4 differences above 10 ppb (Fig. 2 lower panels). The

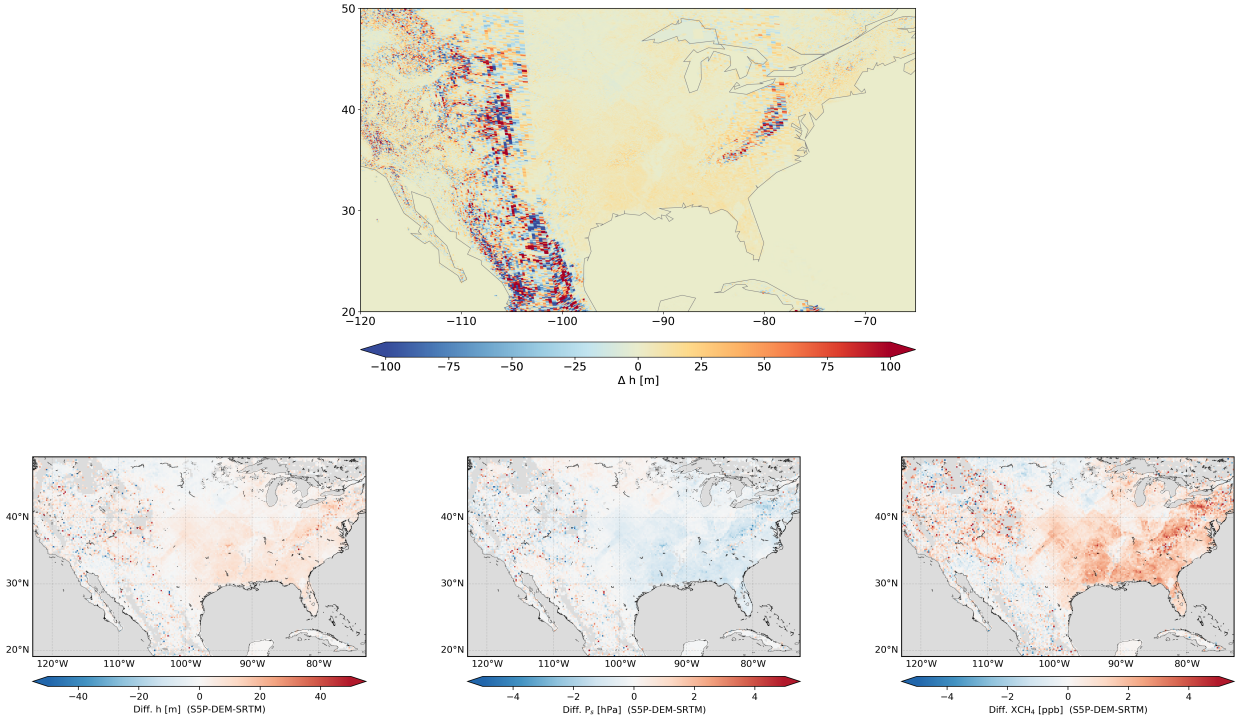

Figure 2. Upper panel: altitude difference between S5P-DEM and SRTM collocated to TROPOMI pixels on 5 May 2019 (orbits 8077, 8078, 8079). Lower panel: altitude, surface pressure and XCH_4 differences averaged over a year, with custom quality filtering for the TROPOMI XCH_4 retrievals, in a 0.2° x 0.2° grid over United States (20-50N, 65-120W).

terrain roughness within TROPOMI pixels has not changed significantly with the SRTM DEM, so it does not affect the data yield due to the 80 m threshold. Although globally the average altitude difference is small, the analysis of small scale XCH_4 enhancements will benefit from this update. Due to its higher resolution the SRTM DEM is a better representation of elevation not only over mountains, but also close to coastlines and over rough terrain (e.g. Greenland, Sahara desert).

3.4 Posteriori correction

Greenhouse gas concentrations retrieved from satellite instruments like TROPOMI generally show systematic biases with different instrumental or geophysical parameters. Retrieved CO_2 and CH_4 from GOSAT and OCO-2 are typically corrected for dependencies on goodness of fit, surface albedo or aerosol parameters (e.g. Guerlet et al. (2013), Inoue et al. (2016), Wu et al. (2018)). In the approach that O'Dell et al. (2018) derived for OCO-2 CO_2 retrievals, such parametric bias is part of a more complex correction that also accounts for footprint-level and global biases using a set of four "truth proxies" as a reference.

The comparison of TROPOMI and TCCON XCH_4 measurements shows a dependence of the bias (i.e. difference between TROPOMI and TCCON) on surface albedo retrieved in the SWIR spectral range, while for the other retrieved parameters the

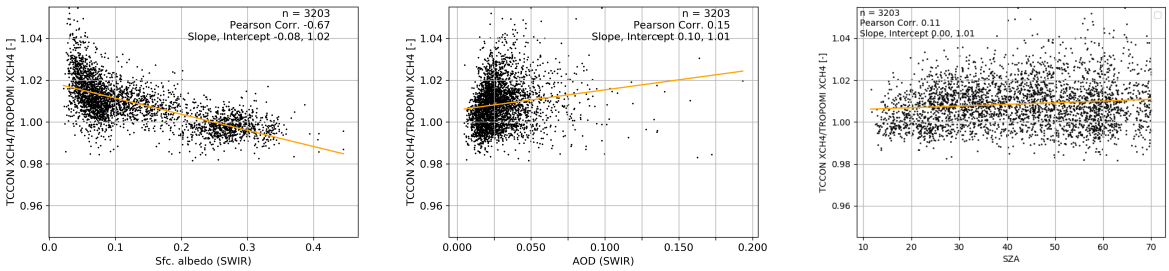

(a) (b) (c)

Figure 3. Ratio of XCH_4 measurements by TCCON and TROPOMI as a function of (a) retrieved surface albedo in the SWIR spectral range, (b) retrieved effective aerosol optical depth (AOD) in SWIR spectral range and (c) solar zenith angle (SZA).

dependence is negligible (compared to that of the surface albedo, see Fig. 3 with solar zenith angle and aerosol optical depth as an example). Figure 3a shows that for low albedo values, TROPOMI XCH_4 strongly underestimates TCCON measurements, while for relatively high albedo values TROPOMI overestimates TCCON measurements. The comparison of TROPOMI XCH_4 with XCH_4 retrieved from measurements of GOSAT shows the same dependence of the bias with the retrieved surface albedo. For scenes with low albedo values, generally the retrieval's sensitivity is low due to the large measurement noise~~.~~, therefore errors from unaccounted light path modification due to scattering processes can be more significant than for scenes with a relatively higher albedo. For low albedo scenes, this effect leads to an underestimation in the retrieved trace gas (Guerlet et al. (2013); Aben et al. (2007)), resembling the TROPOMI XCH_4 underestimation in Fig. 3a.

To account for the albedo dependence, we apply an a posteriori bias correction to the retrieved XCH_4. In the baseline ~~algorithm~~operational algorithm few months after TROPOMI was operational, we applied a correction based on the comparison of TROPOMI XCH_4 with GOSAT retrievals (Hasekamp et al., 2019). After more than two years of measurements, we have sufficient data to derive ~~the~~ a new correction using only TROPOMI XCH_4 measurements. We use a similar approach to the "small area approximation" applied to OCO-2 (O'Dell et al., 2018), assuming a uniform XCH_4 distribution as a function of albedo in several regions. This approach makes the correction completely independent of any reference data (e.g. GOSAT, TCCON) that could introduce additional biases when applying the correction and does not allow for an independent verification of the correction.

The new correction is derived as follows:

1. We select areas at several latitudes and longitudes throughout the globe, small enough so we can assume that XCH_4 does not vary, but large enough to cover scenes with a wide range of albedo values. Figure B1 shows the different regions.

2. For each region we estimate a XCH_4 reference value for a surface albedo around 0.2 and then we calculate the ratio of the retrieved XCH_4 to the reference value to obtain the albedo dependence. The specific value for surface albedo is selected because XCH_4 retrieval errors are lower in the SWIR for that albedo range: errors because of unaccounted light

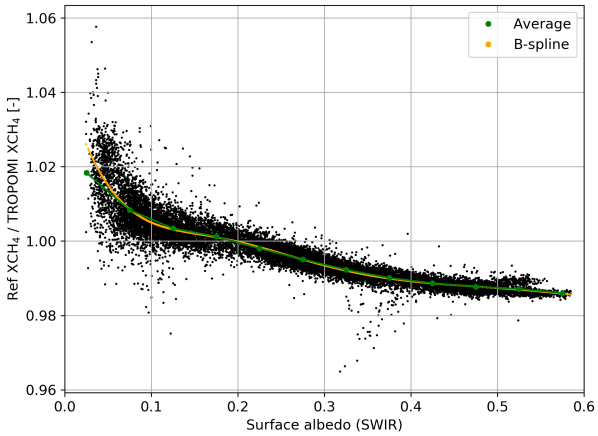

Figure 4. Ratio of reference XCH_4 to TROPOMI XCH_4 as a function of the retrieved surface albedo as explained in step 3 in the derivation of the bias correction. Green dots show the average ratio in 0.05 albedo bins and orange line shows the B-spline fit used to derive the bias correction. Data is averaged from 1 Jan 2018 until 31 Dec 2019 in a 0.1° x 0.1° grid.

path modifications due to scattering and surface albedo are minimal around a surface albedo of 0.2 (e.g. Guerlet et al. (2013); Aben et al. (2007)).

3. We combine the albedo dependence for all the areas, we fit the curve using B-spline interpolation and least squares fitting.

The B-spline method fits piece-wise polynomials that are continuous at the pre-selected knots. The knots and the order of the polynomials are chosen such that the residual RMS of fit residuals is minimum and that the shape of the fit at the edges of the surface albedo range does not vary sharply.

Figure 4 shows the distribution of the reference to TROPOMI XCH_4 ratio for all the areas and the result of the B-spline fit. We observe two distinct features: (1) the strong underestimation for low albedo values (already shown in the TCCON comparison in Fig. 3a), for which the B-spline fit corrects more strongly than the regular polynomial fit that was previously ~~used~~ derived for the operational product and (2) an overestimation for high albedo values, not captured by TCCON due to the limited albedo range values but reported in the TROPOMI and GOSAT comparisons.

The correction applied to the retrieved XCH_4 can be expressed as:

$$\mathrm{XCH}_{4\,i}^{\mathrm{corr}} = \mathrm{XCH}_{4\,i} \cdot f\,(A_{\mathrm{s}\,i}). \tag{6}$$

The correction function f depends on the retrieved surface albedo A_{s} in the SWIR spectral range at each pixel i.

Figure 5 shows the global distribution of XCH_4 before and after applying the correction. Distinctive features that correspond with low and high surface albedo areas are visible in the difference map. After correction, for example, the XCH_4 underestima-

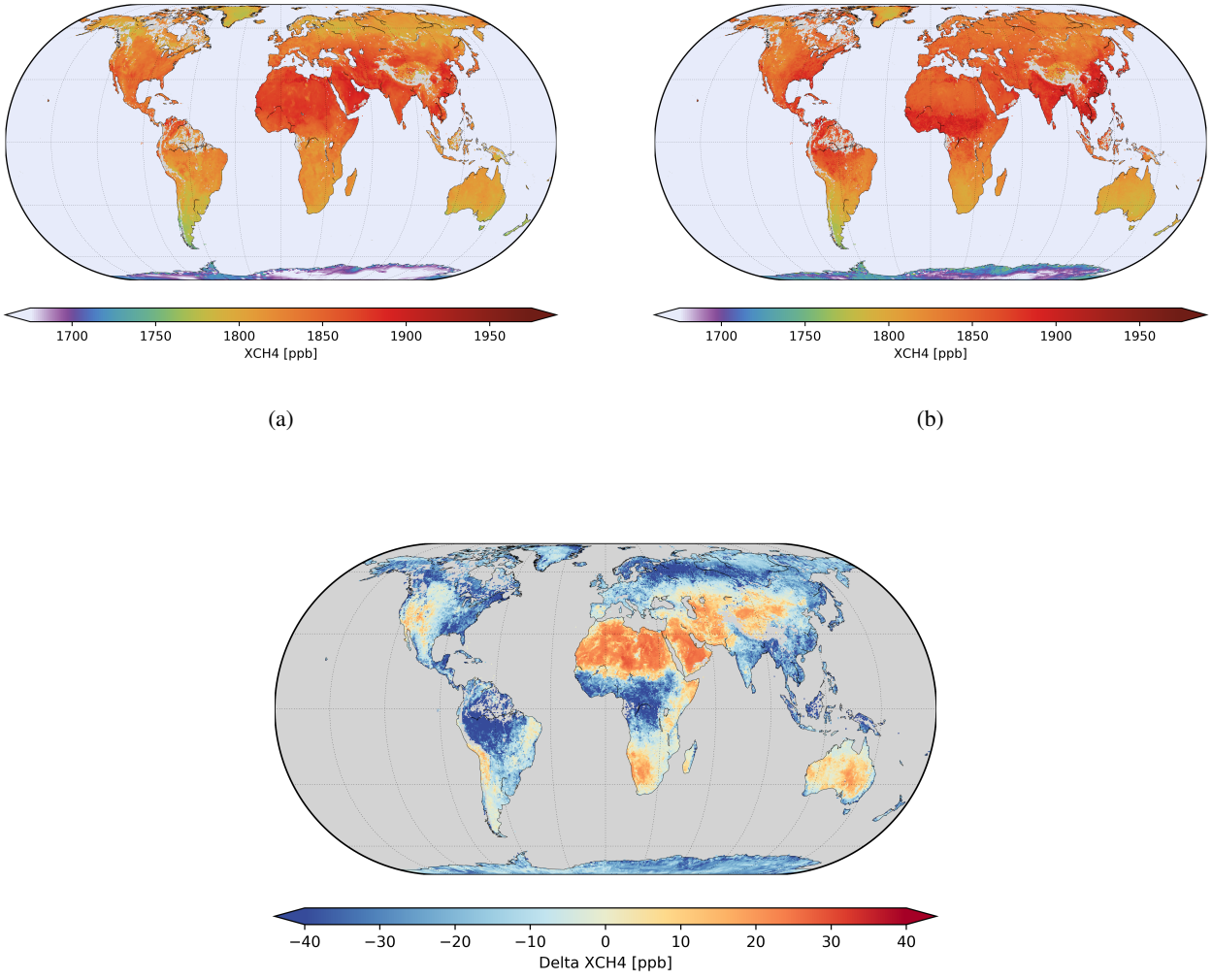

Figure 5. (a) Global TROPOMI XCH_4 distribution before correction, (b) after correction and (c) their difference (XCH_4-XCH_4^{corr}) for 2019 averaged in a cylindrical equal-area grid with 0.3° x 0.5° resolution at the Equator.

tion for low albedo values (e.g. over high latitudes over Canada and Russia) is corrected. Similarly, the XCH_4 overestimation for high albedo values over desert areas like Sahara is accounted for in the correction. The change in XCH_4 induced by the bias correction is in the range of 2 %, in agreement with the errors observed in the TCCON comparison.

As the correction is derived using only TROPOMI XCH_4 data, the comparison with TCCON and GOSAT is an independent verification of the approach. The validation with TCCON shows a reduction of 5.9 ppb (50%) in the station-to-station variability and of 13.6 ppb in the bias due to the albedo correction. The dependence of the bias on surface albedo is removed (Fig. 3a vs.

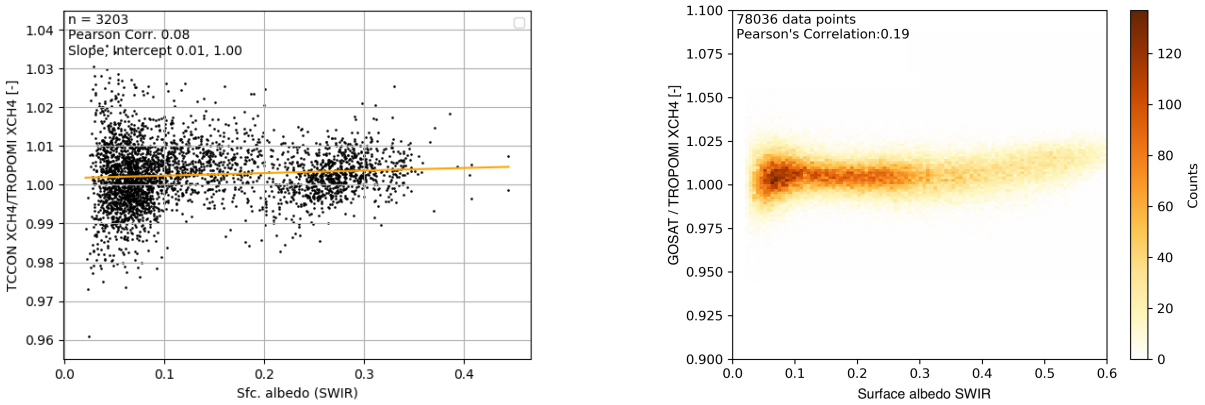

Figure 6. Ratio of daily XCH_4 measurements by (a) TCCON and TROPOMI and (b) GOSAT and TROPOMI as a function of retrieved surface albedo in the SWIR spectral range. Data for the period 1 Dec 2018 - 31 Dec 2019 is shown.

Fig. 6a) and the dependence on other parameters remains negligible (not shown). The comparison with GOSAT measurements shows that bias dependence on albedo is removed after applying the correction (Fig. 6b), which reduces by 4 ppb the scatter of the differences in XCH_4 measured by the two satellites. In the remainder of the paper the corrected XCH_4 product will be used.

4 Comparison of TROPOMI and TCCON

4.1 TCCON validation

We perform a detailed comparison of the TROPOMI XCH_4 corrected with XCH_4 measured at 13 TCCON stations selected for the validation (Table 1). TROPOMI is able to capture the temporal XCH_4 variability, both the seasonal cycle and the year-to-year increase. This is clearly visible in the time series (e.g. Pasadena or Lamont) in Fig. 7, which shows the time series of daily average XCH_4 measured at each TCCON station and by TROPOMI for the period 1 Dec 2018 – 31 Dec 2019, with a collocation radius of 300 km.

The mean bias is below 1 % for all stations; the validation results are summarized in Table 3. The average bias for all stations is -0.2 % (-3.4 ~~pbb~~ppb) and the station to station variability is 0.3% (5.6 ~~pbb~~ppb), both parameters below the mission requirements for TROPOMI XCH_4 retrievals. Compared to the uncorrected TROPOMI XCH_4, the mean bias is reduced significantly (from -3.4 % to 0.2 %) even though the correction approach does not include any term to correct a global bias. As the overall negative bias is driven by the strong XCH_4 underestimation for low albedo values (Fig. 3a), correcting for the albedo bias partly accounts for the overall bias.

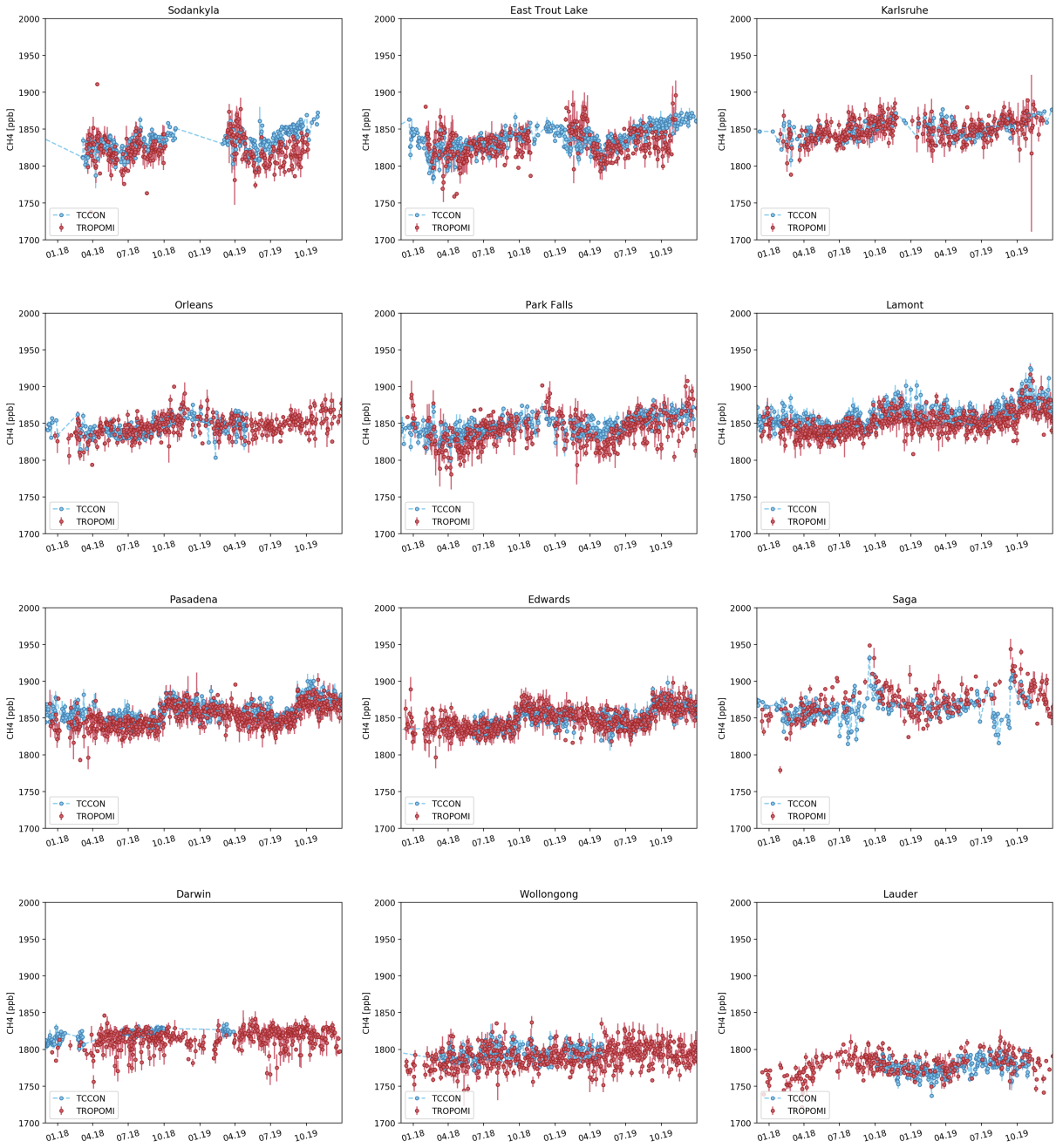

Figure 7. Time series of daily averaged XCH_4 measurements from TROPOMI (red) and TCCON (blue) over the selected stations for the period 1 Dec 2018 – 31 Dec 2019. TROPOMI measurements around a circle of 300 km radius around each station have been selected for the comparison.

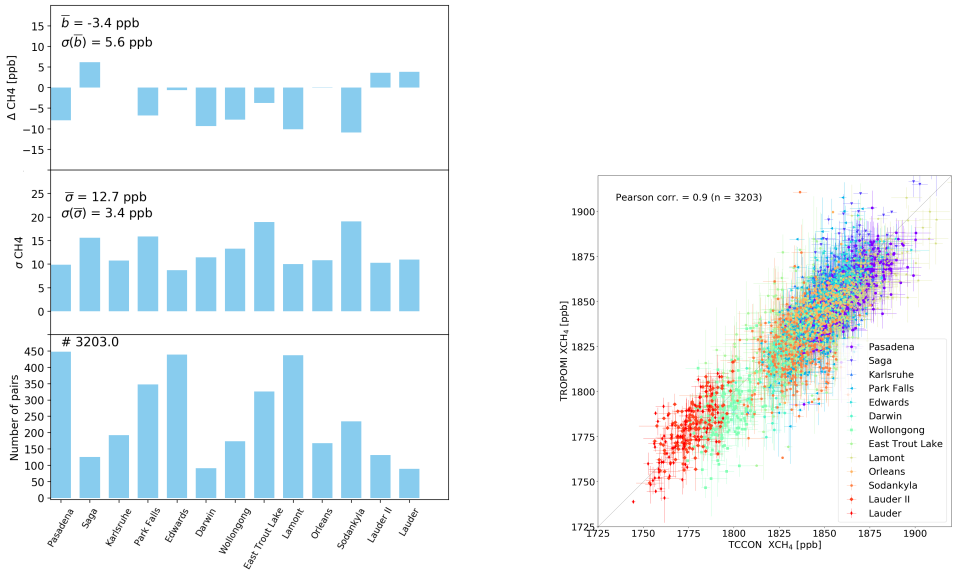

(a) (b)

Figure 8. (a) Mean differences between TROPOMI and TCCON XCH_4 (ΔXCH_4), the standard deviation of the differences (σ_{XCH_4}) and the number of collocations for each of the stations selected for the validation. (b) Correlation of daily average XCH_4 measured by TROPOMI and TCCON for all the stations.

Figure 8a shows the mean bias and the standard deviation for each of the stations and Fig. 8b shows the correlation plot. For a more strict collocation criterion of 100 km radius instead of 300 km, the number of points is reduced significantly but the results of the validation do not change.

4.2 High latitude stations

Measurements at high latitude stations such as East Trout Lake (54.36°N) and Sodankylä (67.37°N) show the highest variability and the highest bias in the validation before correction, which is partially reduced by the albedo correction (see validation results in Table 3). There is a seasonality in the bias which is positive during February – April period and changes to a negative bias around May that then increases to reach the highest (negative) values in fall. This seasonality can be attributed to the fact that during the winter there is snow in these regions at high latitudes as a result of cold, dry air, influencing XCH_4 measurements by TROPOMI that affect the validation with TCCON measurements.

Figure 9 shows the time series of the bias between TROPOMI and TCCON XCH_4 together with the surface albedo retrieved in both the SWIR and NIR spectral range over East Trout Lake, Sodankylä and Lamont, the latter included as a mid-latitude reference. Low surface albedo in the SWIR together with high surface albedo in the NIR indicates the presence of snow which is highly correlated with the seasonality in the bias in East Trout Lake and Sodankylä, seasonality that is more pronounced in 2019 than 2018. The seasonal bias is also correlated with high hydrogen fluoride (HF) and low H_2O concentrations (not

Table 3. Overview of the validation results of TROPOMI XCH_4 with measurements from the TCCON network at selected stations. The table shows number of collocations, mean bias and standard deviation for each station and the mean bias for all stations and the station-to-station variability (in ppb and in percentages between parenthesis). Results are shown for TROPOMI XCH_4 with and without the albedo bias correction applied.

		Corrected TROPOMI XCH_4 and TCCON		**Uncorrected TROPOMI XCH_4 and TCCON**	
Site, Country, Lat-Lon Coord.	**Nr. of points**	**Bias [ppb] (%)**	**Standard deviation [ppb] (%)**	**Bias [ppb] (%)**	**Standard deviation [ppb] (%)**
Pasadena (US) (34.14, −118.13)	399	−8.0 (−0.4)	9.8 (0.5)	0.6 (0.03)	9.3 (0.5)
Saga (Japan) (33.24, 130.29)	117	6.2 (0.3)	15.6 (0.8)	−17.6 (−0.9)	13.0 (0.7)
Karlsruhe (Germany) (49.1, 8.44)	196	0.02 (0.0)	10.8 (0.6)	-19.2 (−1.0)	10.1 (0.5)
Darwin (Australia) (−12.46, 130.93)	93	−9.3 (−0.5)	11.4 (0.6)	−16.5 (−0.9)	11.8 (0.7)
Wollongong (Australia) (−34.41, 150.88)	132	−7.8 (−0.4)	13.3 (0.7)	−19.6 (−1.1)	14.9 (0.8)
Lauder I (New Zealand) (−45.04, 169.68)	99	3.6 (0.2)	10.3 (0.6)	−12.3 (−0.7)	10.4 (0.6)
Lauder II (New Zealand) (−45.04, 169.68)	93	3.8 (0.2)	11.0 (0.6)	−11.8 (−0.67)	10.8 (0.6)
Park Falls (US) (45.94, -90.27)	325	−6.8 (−0.4)	15.9 (0.9)	−29.3 (−1.6)	17.4 (0.9)
East Trout Lake (Canada) (54.36, −104.99)	315	−3.7 (−0.2)	19.0 (1.0)	−27.1 (−1.5)	21.4 (1.2)
Lamont (US) (36.6, −97.49)	388	−10.1 (−0.5)	10.0 (0.5)	−19.6 (−1.1)	11.2 (0.6)
Orléans (France) (47.97, 2.11)	139	−0.07 (0.0)	10.8 (0.6)	−16.0(−0.9)	12.0 (0.7)
Edwards (US) (34.95, −117.88)	373	−0.6 (−0.03)	8.7 (0.5)	7.1 (0.4)	8.8 (0.5)
Sodankylä (Finland) (67.37, 26.63)	234	−10.9 (−0.6)	19.1 (1.0)	−39.4 (−2.1)	18.6 (1.0)
Mean bias, station-to-station variability		−3.4 (−0.2)	5.6 (0.3)	−17.0 (-0.9)	11.5 (0.6)

shown). High HF concentrations are an indication of the influence of the vortex in a specific location, as HF is mostly found in the stratosphere; HF together with the contrast between surface albedo retrieved in the SWIR and NIR spectral ranges can be used as a proxy to identify the presence of snow and dry air from dynamic meteorological situations at high latitudes.

The presence of snow at high latitude stations shifts the focus to retrieval errors as the most probable cause of the seasonal bias between TCCON and TROPOMI, rather than errors due to collocation or influence of the different priors. Scenes covered by snow are characterized by low spectrum intensity in the SWIR, so signal-to-noise ratio is a limiting factor. On the other hand, the high TROPOMI signal in the NIR suggests that the weighting of each band might not be optimal in the inversion. As the optical properties are different in the NIR and SWIR bands, errors in the quantification of light path modifications over snow covered scenes can lead to an overestimation of retrieved XCH_4. Furthermore, if H_2O may compensate for any radiometric offset in the strong CH_4 absorption bands, then in such dry conditions this would not be as effective in winter as

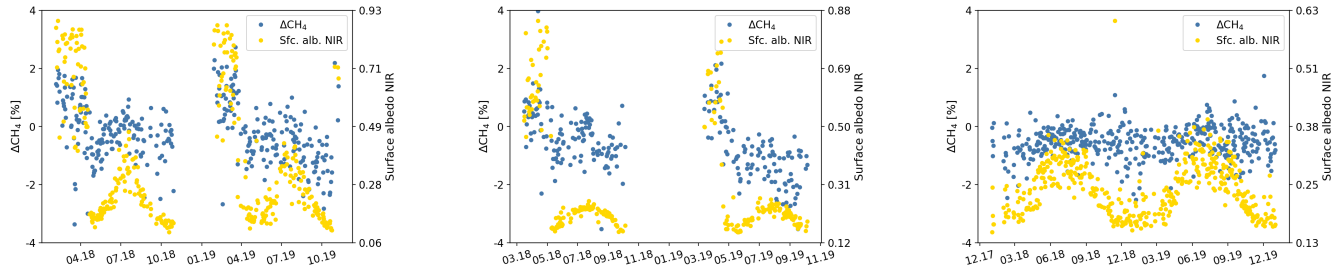

(a) East Trout Lake, NIR (c) Sodankylä, NIR (e) Lamont, NIR

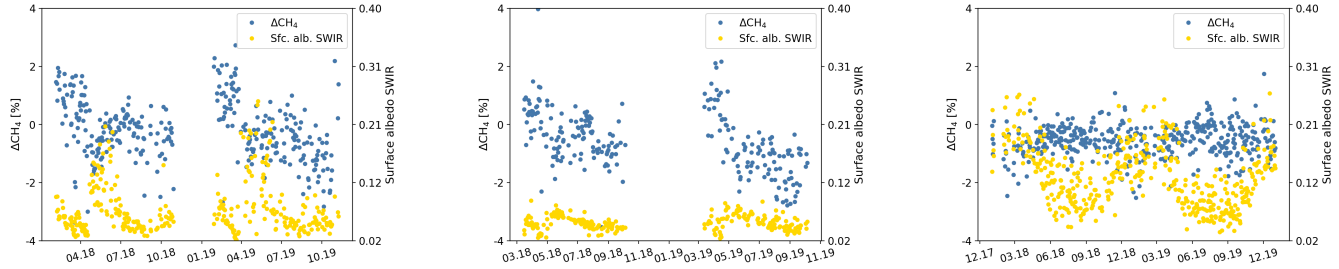

(b) East Trout Lake, SWIR (d) Sodankylä, SWIR (f) Lamont, SWIR

Figure 9. Daily mean relative differences (blue, left axis) between TROPOMI and TCCON XCH_4 (ΔCH_4) and surface albedo in the NIR (yellow, secondary axis, first row) and surface albedo in the SWIR (yellow, secondary axis, second row) at East Trout Lake (54.3°N) (first column), Sodankylä (67.4°N) (second column) and Lamont (36.6°N) (third column).

in spring–fall, causing the seasonality on the bias. A high bias in high latitudes correlated with H_2O columns was also found in H_2O/HDO retrievals from TROPOMI by Schneider et al. (2020). Note that the seasonal bias is also present when XCH_4 is retrieved using the spectroscopic databases discussed in Sect. 3.2.

To filter for scenes covered with snow or ice, Wunch et al. (2011b) introduced the so-called "blended-albedo", which combines the surface albedo in the NIR and SWIR to be used as a filter. By applying it to Sodankylä and East Trout Lake, we found that a threshold value of 0.85 is optimal to remove these scenes that cause the seasonality on the bias. The influence of snow needs to be further investigated from the retrieval algorithm perspective, and it should be considered when interpreting the validation results and when analysing TROPOMI XCH_4 data over snow-covered scenes, most prevalent at high latitudes.

5 Comparison with GOSAT satellite

We compare XCH_4 retrieved from TROPOMI and GOSAT measurements for a period of two years (Jan 2018 – Dec 2019). The comparison yields a mean bias of -10.3 ± 16.8 ppb (-0.6 ± 0.9 %) and a Pearson's correlation coefficient of 0.85. The overall comparison yields a mean bias of -12.5 ± 14.9 ppb if we use the GOSAT XCH_4 product retrieved with the full-physics approach. Figure 10 shows TROPOMI and GOSAT XCH_4 and their ratio averaged to a 2°x 2° grid. Overall compared to GOSAT, TROPOMI underestimates XCH_4, specially in the regions around the tropics in South America (-0.6 ± 0.8 %) and

in the African continent (-0.9 ± 0.8 %). In Asia there is higher variability (up to 1 %) compared to other regions, with areas of underestimation as well as overestimation. The overall underestimation is stronger by about 2 % in the non-corrected XCH_4, reflecting that the albedo correction improves the too low TROPOMI XCH_4 in areas where the surface albedo is low (e.g. forests around the Equator). For higher latitudes, the underestimation is less strong, and in some areas TROPOMI overestimates XCH_4 compared to GOSAT (e.g. Greenland and Antarctica), in agreement with the high bias in XCH_4 reported in the TCCON validation at East Trout Lake and Sodankylä.

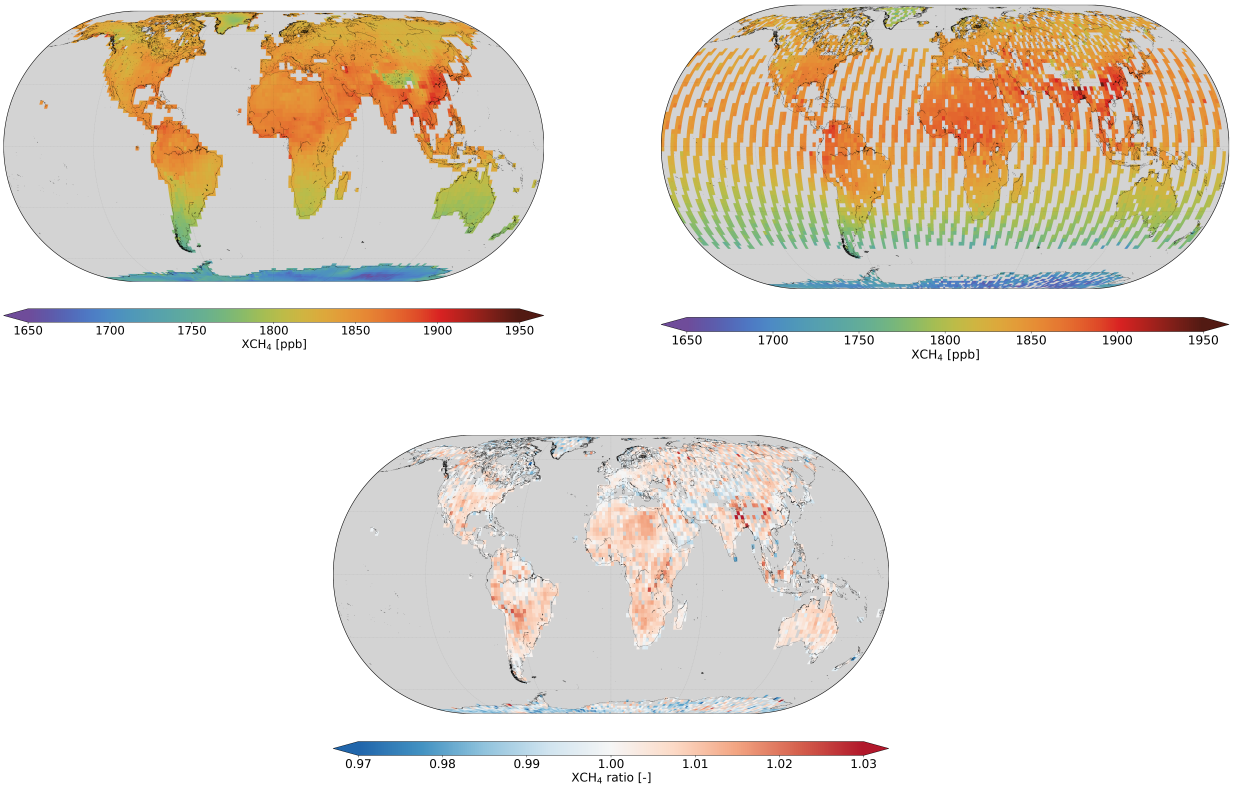

Figure 10. Global distribution of XCH_4 measured by (a) TROPOMI, (b) GOSAT and (c) the ratio of GOSAT to TROPOMI XCH_4. Daily collocations are averaged to a 2°x2° grid for the period 1 Jan 2018 – 31 Dec 2019.

The latitudinal distribution of XCH_4 from TROPOMI, GOSAT and TROPOMI collocated with TCCON stations is shown in Fig. 11, summarising the validation of TROPOMI XCH_4 and showing the good agreement between the three datasets. Similar to Fig. 10, it shows that TROPOMI underestimates GOSAT at most latitudes but both overlap within the XCH_4 variability. It also shows the shift to an overestimation at high latitudes where TROPOMI retrieves higher XCH_4. This agrees with the conclusion that over snow TROPOMI XCH_4 is too high and although this distribution resembles the latitudinal distribution of XCH_4 shown in Fig. 1, it cannot be attributed to the selection of the spectroscopic database.

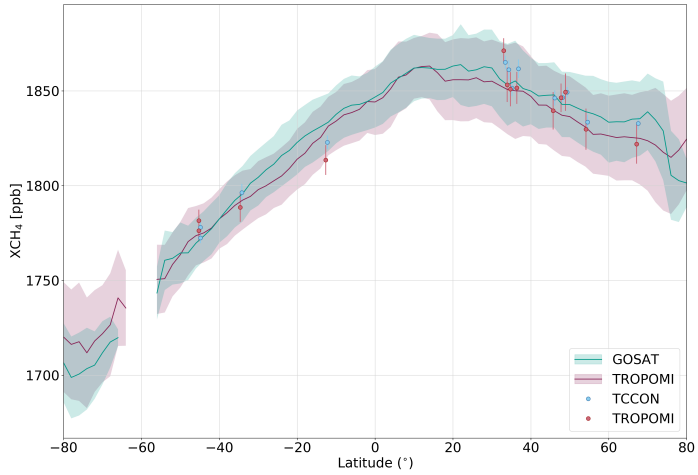

Figure 11. Latitudinal distribution of XCH_4 measured by TROPOMI and GOSAT, and the TROPOMI and TCCON collocations over the selected stations for validation in Sect. 4. The shaded bands indicate the scatter (i.e. 1σ standard deviation) around the mean.

6 Conclusions

We have presented several improvements that have been implemented in the retrieval of XCH_4 from TROPOMI measurements in the NIR and SWIR spectral range. Now that TROPOMI has been measuring for more than two years, the amount of data allows the implementation of a series of updates that were not previously possible without the use of any reference data (i.e. regularization scheme and a posteriori correction derived using only TROPOMI XCH_4 data).

The regularization scheme with constant regularization parameters stabilizes the retrieval and yields less scatter in the TROPOMI XCH_4 data compared to the operational data product (version 1.2.0 Hu et al. (2016)). We have investigated the effect of the horizontal resolution of the surface elevation database by replacing GMTED2010 S5P with the SRTM 15" database, relevant in the XCH_4 retrieval for which accurate knowledge of surface pressure is necessary. The higher resolution database results in a more realistic representation of surface altitude, particularly for mountainous regions and places with rough surfaces, where differences in surface pressure above 5 hPa result in retrieved XCH_4 that varies up to 10 ppb for specific scenes.

We have tested three state-of-the-art spectroscopic databases (HITRAN 2008 with updates from Scheepmaker et al. (2013), HITRAN 2016 and SEOM-IAS). Using the SEOM-IAS database results in the best spectral fitting quality parameters in the retrieved XCH_4. Each of the different spectroscopic database introduces a bias in the distribution of XCH_4 with respect to each other, but there is not any additional bias (e.g. latitudinal, albedo bias) that could point to the fitness for purpose of any of the databases. In view of the best fitting results, we decided to use the SEOM-IAS database, which was derived specifically for TROPOMI. However, there is a need for a thorough and detailed analysis of these databases focusing on the different absorbers that are relevant in the CH_4 absorption bands to learn about the underlying processes that are driving the overall bias.

One of the most relevant updates is the implementation of a posteriori correction that is fully independent of any reference data. We have derived a correction for the bias dependence on albedo using only TROPOMI XCH_4 data. This has been possible due to the high resolution of TROPOMI and its global coverage. We select regions around the globe which cover different albedo ranges and dependencies to estimate the albedo bias. The new correction is more accurate than the regular polynomial fit for the strong XCH_4 underestimation at low surface albedo scenes, and also corrects for the positive bias in scenes with high surface albedo. After applying the correction, the albedo dependence in the TROPOMI-GOSAT and TROPOMI-TCCON comparison is removed, which is an independent verification of the correction scheme. The change in XCH_4 induced by the bias correction is in the range of 2 %, and although we attribute it mostly to unaccounted light path modification due to scattering processes, Butz et al. (2012) predicted residual scattering errors to be mostly below 1 % which suggests that other errors might exist that needs to be further investigated.

The good agreement of TROPOMI XCH_4 with TCCON (-3.4 ± 5.6 ppb) and GOSAT (-10.3 ± 16.8 ~~pbb~~ppb) highlights the high quality of the TROPOMI measurements. Low and high albedo scenes are the most challenging for the XCH_4 retrieval algorithm, and although the posteriori correction accounts for most of the bias, there is a need to further understand the underlying cause and whether it originates in the instrument or in the retrieval algorithm. Also the overestimation of XCH_4 over snow covered scenes requires further investigation from the retrieval algorithm perspective. With respect to the validation, additional sites would be beneficial to cover the under-sampled regions and conditions. The network is currently limited to relatively low albedo values, so there is a lack of reference data for high albedo scenes, particularly around the Equator. Furthermore, there is a clear imbalance between the number of stations in the Northern and Southern hemisphere, as well as a lack of stations below 45° S. This is not only relevant for a complete validation of current and future satellite instruments, but also to have a complete global network to monitor concentrations of CH_4 in the atmosphere.

Appendix A: Filtering criteria

Table A1. Overview of the filters applied to assure high-quality TROPOMI XCH_4 retrievals.

Parameter	Range
Cloud fraction* from VIIRS inner field of view (IFOV)	< 0.001
Cloud fraction* from VIIRS outer field of view (OFOV) (upscaled FOV by 10, 50 and 100%) (OFOVa, b, c)	< 0.001
Ratio of XCH_4 retrieved from strong and weak absorption bands with the non-scattering retrieval using H2016 cross-sections	0.85< x< 1.15
Standard deviation of XCH_4 ratio within SWIR pixel plus 8 neighbouring pixels	< 0.05
Signal-to-noise ratio	> 50
Precision (noise-related error)	< 10
χ^2	< 100
Retrieved AOT (SWIR)	< ~~0.3~~ 0.1
Surface albedo	> 0.02
Solar zenith angle (°)	< 70
Viewing zenith angle (°)	< 60
Terrain roughness (m) Standard deviation of surface elevation within ground pixel	< 80

* Cloud fraction defined as fraction of VIIRS pixels classified as confidently clear sky.

Appendix B: Regions selected for the posteriori correction

The regions selected to estimate the posteriori correction are shown in Fig. B1.

Data availability. The TROPOMI CH_4 dataset of this study is available for download at ftp://ftp.sron.nl/open-access-data-2/TROPOMI/tropomi/ch4/ (last access: 26 June 2019). TCCON data are available from the TCCON Data Archive, hosted by CaltechDATA, California Institute of Technology, CA (US), https: //tccondata.org/ (TCCON, 2020).

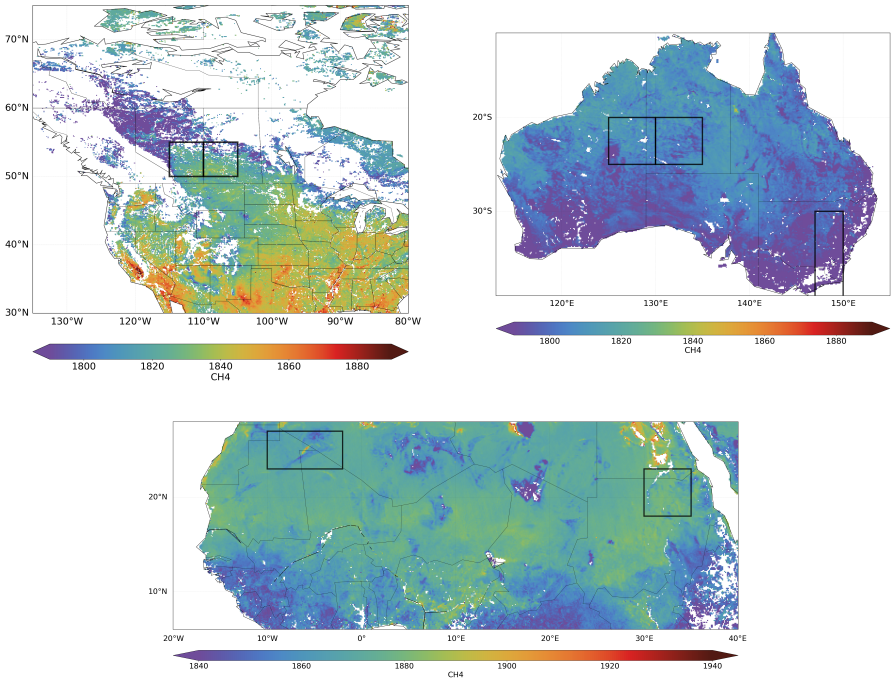

Figure B1. Black boxes over North Africa, Australia and Canada correspond to the different regions selected to estimate the posteriori correction (see Sect. 3.4). Global distribution of XCH_4 averaged to a 0.1°x 0.1° grid for the period 1 Jan 2018 - 31 Dec 2019.

Author contributions. AL, TB, OH, JdB, AS, AB and JL provided the TROPOMI CH_4 retrieval and data analysis. The TCCON partners provided the validation datasets. AL wrote the original draft with input from TB and JL, all authors discussed the results and review and edited the manuscript.

Competing interests. The authors declare that they have no conflict of interest.

Disclaimer. The presented work has been performed in the frame of Sentinel-5 Precursor Validation Team (S5PVT) or Level 1/Level 2 Product Working Group activities. Results are based on preliminary (not fully calibrated or validated) Sentinel-5 Precursor data that will still change. The results are based on S5P L1B version 1 data. Plots and data contain modified Copernicus Sentinel data, processed by SRON.

Acknowledgements. The TROPOMI data processing was carried out on the Dutch National e-infrastructure with the support of the SURF Cooperative. Funding through the TROPOMI national program from the NSO and Methane+ is acknowledged. Darwin and Wollongong TCCON sites are funded by the Australian Research Council (DP140101552, DP160101598, LE0668470) and NASA (NAG5-12247, NNG05-GD07G). NMD is supported by an ARC Future Fellowship FT180100327.

References

Aben, I., Hasekamp, O., and Hartmann, W.: Uncertainties in the space-based measurements of CO_2 columns due to scattering in the Earth's atmosphere, Journal of Quantitative Spectroscopy and Radiative Transfer, 104, 450–459, https://doi.org/https://doi.org/10.1016/j.jqsrt.2006.09.013, 2007.

Barré, J., Aben, I., Agustí-Panareda, A., Balsamo, G., Bousserez, N., Dueben, P., Engelen, R., Inness, A., Lorente, A., McNorton, J., Peuch, V.-H., Radnoti, G., and Ribas, R.: Systematic detection of local CH_4 emissions anomalies combining satellite measurements and high-resolution forecasts, Atmospheric Chemistry and Physics Discussions, 2020, 1–25, https://doi.org/10.5194/acp-2020-550, https://acp.copernicus.org/preprints/acp-2020-550/, 2020.

Birk, M., Wagner, G., Loos, J., Wilzewski, J., Mondelain, D., Campargue, A., Hase, F., Orphal, J., Perrin, A., Tran, H., Daumont, L., Rotger-Languereau, M., Bigazzi, A., and Zehner, C.: Methane and water spectroscopic database for TROPOMI Sentinel 5 Precursor in the 2.3μm region, vol. 19, p. 4652, EGU General Assembly, 2017.

Borsdorff, T., aan de Brugh, J., Schneider, A., Lorente, A., Birk, M., Wagner, G., Kivi, R., Hase, F., Feist, D. G., Sussmann, R., Rettinger, M., Wunch, D., Warneke, T., and Landgraf, J.: Improving the TROPOMI CO data product: update of the spectroscopic database and destriping of single orbits, Atmospheric Measurement Techniques, 12, 5443–5455, https://doi.org/10.5194/amt-12-5443-2019, https://www.atmos-meas-tech.net/12/5443/2019/, 2019.

Buchwitz, M., Reuter, M., Schneising, O., Hewson, W., Detmers, R. G., Boesch, H., Hasekamp, O., Aben, I., Bovensmann, H., Burrows, J., Butz, A., Chevallier, F., Dils, B., Frankenberg, C., Heymann, J., Lichtenberg, G., De Mazière, M., Notholt, J., Parker, R., Warneke, T., Zehner, C., Griffith, D. W. T., Deutscher, N., Kuze, A., Suto, H., and Wunch, D.: Global satellite observations of column-averaged carbon dioxide and methane: The GHG-CCI XCO_2 and XCH_4 CRDP3 data set, Remote Sensing of Environment, 203, 276 – 295, https://doi.org/https://doi.org/10.1016/j.rse.2016.12.027, http://www.sciencedirect.com/science/article/pii/S0034425716305065, earth Observation of Essential Climate Variables, 2017.

Buchwitz, M., Aben, I., Armante, R., Boesch, H., Crevoisier, C., Di Noia, A., Hasekamp, O. P., Reuter, M., Schneising-Weigel, O., and Wu, L.: Algorithm Theoretical Basis Document (ATBD) – Main document for Greenhouse Gas (GHG: CO_2 and CH_4) data set CDR 3 (2003-2018), C3S project, 2019.

Butz, A., Guerlet, S., Hasekamp, O., Schepers, D., Galli, A., Aben, I., Frankenberg, C., Hartmann, J.-M., Tran, H., Kuze, A., Keppel-Aleks, G., Toon, G., Wunch, D., Wennberg, P., Deutscher, N., Griffith, D., Macatangay, R., Messerschmidt, J., Notholt, J., and Warneke, T.: Toward accurate CO_2 and CH_4 observations from GOSAT, Geophysical Research Letters, 38, https://doi.org/10.1029/2011GL047888, https://agupubs.onlinelibrary.wiley.com/doi/abs/10.1029/2011GL047888, 2011.

Butz, A., Galli, A., Hasekamp, O., Landgraf, J., Tol, P., and Aben, I.: TROPOMI aboard Sentinel-5 Precursor: Prospective performance of CH_4 retrievals for aerosol and cirrus loaded atmospheres, Remote Sensing of Environment, 120, 267 – 276, https://doi.org/https://doi.org/10.1016/j.rse.2011.05.030, http://www.sciencedirect.com/science/article/pii/S003442571200082X, 2012.

Frankenberg, C., Meirink, J. F., van Weele, M., Platt, U., and Wagner, T.: Assessing Methane Emissions from Global Space-Borne Observations, Science, 308, 1010–1014, https://doi.org/10.1126/science.1106644, https://science.sciencemag.org/content/308/5724/1010, 2005.

Gordon, I., Rothman, L., Hill, C., Kochanov, R., Tan, Y., Bernath, P., Birk, M., Boudon, V., Campargue, A., Chance, K., Drouin, B., Flaud, J.-M., Gamache, R., Hodges, J., Jacquemart, D., Perevalov, V., Perrin, A., Shine, K., Smith, M.-A., Tennyson, J., Toon, G., Tran, H., Tyuterev, V., Barbe, A., Császár, A., Devi, V., Furtenbacher, T., Harrison, J., Hartmann, J.-M., Jolly, A., Johnson, T., Karman, T., Kleiner, I., Kyuberis, A., Loos, J., Lyulin, O., Massie, S., Mikhailenko, S., Moazzen-Ahmadi, N., Müller, H., Naumenko, O., Nikitin, A., Polyansky,

O., Rey, M., Rotger, M., Sharpe, S., Sung, K., Starikova, E., Tashkun, S., Auwera, J. V., Wagner, G., Wilzewski, J., Wcisło, P., Yu, S., and Zak, E.: The HITRAN 2016 molecular spectroscopic database, Journal of Quantitative Spectroscopy and Radiative Transfer, 203, 3 – 69, https://doi.org/https://doi.org/10.1016/j.jqsrt.2017.06.038, hITRAN2016 Special Issue, 2017.

Griffith, D. W. T., Deutscher, N. M., Velazco, V. A., Wennberg, P. O., Yavin, Y., Keppel-Aleks, G., Washenfelder, R. A., Toon, G. C., Blavier, J.-F., Paton-Walsh, C., Jones, N. B., Kettlewell, G. C., Connor, B. J., Macatangay, R. C., Roehl, C., Ryczek, M., Glowacki, J., Culgan, T., and Bryant, G. W.: TCCON data from Darwin (AU), Release GGG2014.R0, https://doi.org/doi:10.14291/tccon.ggg2014.darwin01.r0/1149290, 2017a.

Griffith, D. W. T., Velazco, V. A., Deutscher, N. M., Paton-Walsh, C., Jones, N. B., Wilson, S. R., Macatangay, R. C., Kettlewell, G. C., Buchholz, R. R., and Riggenbach, M.: TCCON data from Wollongong (AU), Release GGG2014.R0, https://doi.org/doi:10.14291/tccon.ggg2014.wollongong01.r0/1149291, 2017b.

Guerlet, S., Butz, A., Schepers, D., Basu, S., Hasekamp, O. P., Kuze, A., Yokota, T., Blavier, J., Deutscher, N. M., Griffith, D. W., Hase, F., Kyro, E., Morino, I., Sherlock, V., Sussmann, R., Galli, A., and Aben, I.: Impact of aerosol and thin cirrus on retrieving and validating XCO_2 from GOSAT shortwave infrared measurements, Journal of Geophysical Research: Atmospheres, 118, 4887–4905, https://doi.org/10.1002/jgrd.50332, https://doi.org/10.1002/jgrd.50332, 2013.

Hase, F., Blumenstock, T., Dohe, S., Groß, J., and Kiel, M.: TCCON data from Karlsruhe (DE), Release GGG2014.R0, https://doi.org/doi:10.14291/tccon.ggg2014.karlsruhe01.r0/1149270, 2017.

Hasekamp, O., Lorente, A., Hu, H., Butz, A., aan de Brugh, J., and Landgraf, J.: Algorithm Theoretical Baseline Document for Sentinel-5 Precursor methane retrieval, http://www.tropomi.eu/documents/atbd/, 2019.

Hu, H., Hasekamp, O., Butz, A., Galli, A., Landgraf, J., Aan de Brugh, J., Borsdorff, T., Scheepmaker, R., and Aben, I.: The operational methane retrieval algorithm for TROPOMI, Atmospheric Measurement Techniques, 9, 5423–5440, https://doi.org/10.5194/amt-9-5423-2016, https://www.atmos-meas-tech.net/9/5423/2016/, 2016.

Hu, H., Landgraf, J., Detmers, R., Borsdorff, T., Aan de Brugh, J., Aben, I., Butz, A., and Hasekamp, O.: Toward Global Mapping of Methane With TROPOMI: First Results and Intersatellite Comparison to GOSAT, Geophysical Research Letters, 45, 3682–3689, https://doi.org/10.1002/2018GL077259, https://agupubs.onlinelibrary.wiley.com/doi/abs/10.1002/2018GL077259, 2018.

Inoue, M., Morino, I., Uchino, O., Nakatsuru, T., Yoshida, Y., Yokota, T., Wunch, D., Wennberg, P. O., Roehl, C. M., Griffith, D. W. T., Velazco, V. A., Deutscher, N. M., Warneke, T., Notholt, J., Robinson, J., Sherlock, V., Hase, F., Blumenstock, T., Rettinger, M., Sussmann, R., Kyrö, E., Kivi, R., Shiomi, K., Kawakami, S., De Mazière, M., Arnold, S. G., Feist, D. G., Barrow, E. A., Barney, J., Dubey, M., Schneider, M., Iraci, L. T., Podolske, J. R., Hillyard, P. W., Machida, T., Sawa, Y., Tsuboi, K., Matsueda, H., Sweeney, C., Tans, P. P., Andrews, A. E., Biraud, S. C., Fukuyama, Y., Pittman, J. V., Kort, E. A., and Tanaka, T.: Bias corrections of GOSAT SWIR XCO_2 and XCH_4 with TCCON data and their evaluation using aircraft measurement data, Atmospheric Measurement Techniques, 9, 3491–3512, https://doi.org/10.5194/amt-9-3491-2016, https://www.atmos-meas-tech.net/9/3491/2016/, 2016.

Iraci, L. T., Podolske, J. R., Hillyard, P. W., Roehl, C., Wennberg, P. O., Blavier, J.-F., Landeros, J., Allen, N., Wunch, D., Zavaleta, J., Quigley, E., Osterman, G. B., Albertson, R., Dunwoody, K., and Boyden, H.: TCCON data from Edwards (US), Release GGG2014.R1, https://doi.org/10.14291/TCCON.GGG2014.EDWARDS01.R1/1255068, 2016.

Kawakami, S., Ohyama, H., Arai, K., Okumura, H., Taura, C., Fukamachi, T., and Sakashita, M.: TCCON data from Saga (JP), Release GGG2014.R0, https://doi.org/doi:10.14291/tccon.ggg2014.saga01.r0/1149283, 2017.

Kivi, R. and Heikkinen, P.: Fourier transform spectrometer measurements of column CO_2 at Sodankylä, Finland, Geoscientific Instrumentation, Methods and Data Systems, 5, 271–279, https://doi.org/10.5194/gi-5-271-2016, https://gi.copernicus.org/articles/5/271/2016/, 2016.

Kivi, R., Heikkinen, P., and Kyrö, E.: TCCON data from Sodankylä (FI), Release GGG2014.R0, https://doi.org/doi:10.14291/tccon.ggg2014.sodankyla01.r0/1149280, 2017.

Landgraf, J., Hasekamp, O. P., Box, M. A., and Trautmann, T.: A linearized radiative transfer model for ozone profile retrieval using the analytical forward-adjoint perturbation theory approach, Journal of Geophysical Research: Atmospheres, 106, 27 291–27 305, https://doi.org/10.1029/2001JD000636, https://agupubs.onlinelibrary.wiley.com/doi/abs/10.1029/2001JD000636, 2001.

Landgraf, J., Butz, A., Hasekamp, O., Hu, H., and aan de Brugh, J.: Sentinel 5 L2 Prototype Processors, Algorithm Theoretical Baseline Document: Methane Retrieval, 2019.

Lunt, M. F., Palmer, P. I., Feng, L., Taylor, C. M., Boesch, H., and Parker, R. J.: An increase in methane emissions from tropical Africa between 2010 and 2016 inferred from satellite data, Atmospheric Chemistry and Physics, 19, 14 721–14 740, https://doi.org/10.5194/acp-19-14721-2019, https://www.atmos-chem-phys.net/19/14721/2019/, 2019.

Maasakkers, J. D., Jacob, D. J., Sulprizio, M. P., Scarpelli, T. R., Nesser, H., Sheng, J.-X., Zhang, Y., Hersher, M., Bloom, A. A., Bowman, K. W., Worden, J. R., Janssens-Maenhout, G., and Parker, R. J.: Global distribution of methane emissions, emission trends, and OH concentrations and trends inferred from an inversion of GOSAT satellite data for 2010–2015, Atmospheric Chemistry and Physics, 19, 7859–7881, https://doi.org/10.5194/acp-19-7859-2019, https://www.atmos-chem-phys.net/19/7859/2019/, 2019.

Miller, S. M., Michalak, A. M., Detmers, R. G., Hasekamp, O. P., Bruhwiler, L. M. P., and Schwietzke, S.: China's coal mine methane regulations have not curbed growing emissions, Nature Communications, 10, 303, https://doi.org/10.1038/s41467-018-07891-7, https://doi.org/10.1038/s41467-018-07891-7, 2019.

O'Dell, C. W., Eldering, A., Wennberg, P. O., Crisp, D., Gunson, M. R., Fisher, B., Frankenberg, C., Kiel, M., Lindqvist, H., Mandrake, L., Merrelli, A., Natraj, V., Nelson, R. R., Osterman, G. B., Payne, V. H., Taylor, T. E., Wunch, D., Drouin, B. J., Oyafuso, F., Chang, A., McDuffie, J., Smyth, M., Baker, D. F., Basu, S., Chevallier, F., Crowell, S. M. R., Feng, L., Palmer, P. I., Dubey, M., García, O. E., Griffith, D. W. T., Hase, F., Iraci, L. T., Kivi, R., Morino, I., Notholt, J., Ohyama, H., Petri, C., Roehl, C. M., Sha, M. K., Strong, K., Sussmann, R., Te, Y., Uchino, O., and Velazco, V. A.: Improved retrievals of carbon dioxide from Orbiting Carbon Observatory-2 with the version 8 ACOS algorithm, Atmospheric Measurement Techniques, 11, 6539–6576, https://doi.org/10.5194/amt-11-6539-2018, https://www.atmos-meas-tech.net/11/6539/2018/, 2018.

Pandey, S., Gautam, R., Houweling, S., van der Gon, H. D., Sadavarte, P., Borsdorff, T., Hasekamp, O., Landgraf, J., Tol, P., van Kempen, T., Hoogeveen, R., van Hees, R., Hamburg, S. P., Maasakkers, J. D., and Aben, I.: Satellite observations reveal extreme methane leakage from a natural gas well blowout, Proceedings of the National Academy of Sciences, 116, 26 376–26 381, https://doi.org/10.1073/pnas.1908712116, https://www.pnas.org/content/116/52/26376, 2019.

Pollard, D. F., Robinson, J., and Shiona, H.: TCCON data from Lauder (NZ), Release GGG2014.R0, https://doi.org/10.14291/TCCON.GGG2014.LAUDER03.R0, 2019.

Rothman, L., Gordon, I., Barbe, A., Benner, D., Bernath, P., Birk, M., Boudon, V., Brown, L., Campargue, A., Champion, J.-P., Chance, K., Coudert, L., Dana, V., Devi, V., Fally, S., Flaud, J.-M., Gamache, R., Goldman, A., Jacquemart, D., Kleiner, I., Lacome, N., Lafferty, W., Mandin, J.-Y., Massie, S., Mikhailenko, S., Miller, C., Moazzen-Ahmadi, N., Naumenko, O., Nikitin, A., Orphal, J., Perevalov, V., Perrin, A., Predoi-Cross, A., Rinsland, C., Rotger, M., Šimečková, M., Smith, M., Sung, K., Tashkun, S., Tennyson, J., Toth, R., Vandaele, A., and Auwera, J. V.: The HITRAN 2008 molecular spectroscopic database, Journal of Quantitative Spectroscopy and Radiative Transfer, 110, 533 – 572, https://doi.org/https://doi.org/10.1016/j.jqsrt.2009.02.013, hITRAN, 2009.

Saunois, M., Stavert, A. R., Poulter, B., Bousquet, P., Canadell, J. G., Jackson, R. B., Raymond, P. A., Dlugokencky, E. J., Houweling, S., Patra, P. K., Ciais, P., Arora, V. K., Bastviken, D., Bergamaschi, P., Blake, D. R., Brailsford, G., Bruhwiler, L., Carlson, K. M., Carrol,

M., Castaldi, S., Chandra, N., Crevoisier, C., Crill, P. M., Covey, K., Curry, C. L., Etiope, G., Frankenberg, C., Gedney, N., Hegglin, M. I., Höglund-Isaksson, L., Hugelius, G., Ishizawa, M., Ito, A., Janssens-Maenhout, G., Jensen, K. M., Joos, F., Kleinen, T., Krummel, P. B., Langenfelds, R. L., Laruelle, G. G., Liu, L., Machida, T., Maksyutov, S., McDonald, K. C., McNorton, J., Miller, P. A., Melton, J. R., Morino, I., Müller, J., Murgia-Flores, F., Naik, V., Niwa, Y., Noce, S., O'Doherty, S., Parker, R. J., Peng, C., Peng, S., Peters, G. P., Prigent, C., Prinn, R., Ramonet, M., Regnier, P., Riley, W. J., Rosentreter, J. A., Segers, A., Simpson, I. J., Shi, H., Smith, S. J., Steele, L. P., Thornton, B. F., Tian, H., Tohjima, Y., Tubiello, F. N., Tsuruta, A., Viovy, N., Voulgarakis, A., Weber, T. S., van Weele, M., van der Werf, G. R., Weiss, R. F., Worthy, D., Wunch, D., Yin, Y., Yoshida, Y., Zhang, W., Zhang, Z., Zhao, Y., Zheng, B., Zhu, Q., Zhu, Q., and Zhuang, Q.: The Global Methane Budget 2000–2017, Earth System Science Data Discussions, 2019, 1–136, https://doi.org/10.5194/essd-2019-128, https://essd.copernicus.org/preprints/essd-2019-128/, 2019.

Scheepmaker, R. A., Frankenberg, C., Galli, A., Butz, A., Schrijver, H., Deutscher, N. M., Wunch, D., Warneke, T., Fally, S., and Aben, I.: Improved water vapour spectroscopy in the 4174-4300 cm^{-1} region and its impact on SCIAMACHY HDO/H_2O measurements, Atmospheric Measurement Techniques, 6, 879–894, https://doi.org/10.5194/amt-6-879-2013, https://www.atmos-meas-tech.net/6/879/2013/, 2013.

Schepers, D., Guerlet, S., Butz, A., Landgraf, J., Frankenberg, C., Hasekamp, O., Blavier, J.-F., Deutscher, N. M., Griffith, D. W. T., Hase, F., Kyro, E., Morino, I., Sherlock, V., Sussmann, R., and Aben, I.: Methane retrievals from Greenhouse Gases Observing Satellite (GOSAT) shortwave infrared measurements: Performance comparison of proxy and physics retrieval algorithms, Journal of Geophysical Research: Atmospheres, 117, https://doi.org/10.1029/2012JD017549, https://agupubs.onlinelibrary.wiley.com/doi/abs/10.1029/2012JD017549, 2012.

Schepers, D., aan de Brugh, J., Hahne, P., Butz, A., Hasekamp, O., and Landgraf, J.: LINTRAN v2.0: A linearised vector radiative transfer model for efficient simulation of satellite-born nadir-viewing reflection measurements of cloudy atmospheres, Journal of Quantitative Spectroscopy and Radiative Transfer, 149, 347 – 359, https://doi.org/A linearised vector radiative transfer model for efficient simulation of satellite-born nadir-viewing reflection measurements of cloudy atmospheres, 2014.

Schneider, A., Borsdorff, T., aan de Brugh, J., Aemisegger, F., Feist, D. G., Kivi, R., Hase, F., Schneider, M., and Landgraf, J.: First data set of H_2O/HDO columns from the Tropospheric Monitoring Instrument (TROPOMI), Atmospheric Measurement Techniques, 13, 85–100, https://doi.org/10.5194/amt-13-85-2020, https://www.atmos-meas-tech.net/13/85/2020/, 2020.

Schneising, O., Buchwitz, M., Reuter, M., Bovensmann, H., Burrows, J. P., Borsdorff, T., Deutscher, N. M., Feist, D. G., Griffith, D. W. T., Hase, F., Hermans, C., Iraci, L. T., Kivi, R., Landgraf, J., Morino, I., Notholt, J., Petri, C., Pollard, D. F., Roche, S., Shiomi, K., Strong, K., Sussmann, R., Velazco, V. A., Warneke, T., and Wunch, D.: A scientific algorithm to simultaneously retrieve carbon monoxide and methane from TROPOMI onboard Sentinel-5 Precursor, Atmospheric Measurement Techniques, 12, 6771–6802, https://doi.org/10.5194/amt-12-6771-2019, https://amt.copernicus.org/articles/12/6771/2019/, 2019.

Schneising, O., Buchwitz, M., Reuter, M., Vanselow, S., Bovensmann, H., and Burrows, J. P.: Remote sensing of methane leakage from natural gas and petroleum systems revisited, Atmospheric Chemistry and Physics, 20, 9169–9182, https://doi.org/10.5194/acp-20-9169-2020, https://acp.copernicus.org/articles/20/9169/2020/, 2020.

Sherlock, V., Connor, B., Robinson, J., Shiona, H., Smale, D., and Pollard, D. F.: TCCON data from Lauder (NZ), 125HR, Release GGG2014.R0, https://doi.org/doi:10.14291/tccon.ggg2014.lauder02.r0/1149298, 2017.

Turner, A. J., Frankenberg, C., and Kort, E. A.: Interpreting contemporary trends in atmospheric methane, Proceedings of the National Academy of Sciences, 116, 2805–2813, https://doi.org/10.1073/pnas.1814297116, https://www.pnas.org/content/116/8/2805, 2019.

Veefkind, J. P., Aben, I., McMullan, K., Förster, H., de Vries, J., Otter, G., Claas, J., Eskes, H., de Haan, J., Kleipool, Q., van Weele, M., Hasekamp, O., Hoogeveen, R., Landgraf, J., Snel, R., Tol, P., Ingmann, P., Voors, R., Kruizinga, B., Vink, R., Visser, H., and Levelt, P.: TROPOMI on the ESA Sentinel-5 Precursor: A GMES mission for global observations of the atmospheric composition for climate, air quality and ozone layer applications, Remote Sensing of Environment, 120, 70 – 83, https://doi.org/https://doi.org/10.1016/j.rse.2011.09.027, 2012.

Warneke, T., Messerschmidt, J., Notholt, J., Weinzierl, C., Deutscher, N. M., Petri, C., and Grupe, P.: TCCON data from Orléans (FR), Release GGG2014.R0, https://doi.org/doi:10.14291/tccon.ggg2014.orleans01.r0/1149276, 2017.

Wennberg, P. O., Roehl, C. M., Wunch, D., Toon, G. C., Blavier, J.-F., Washenfelder, R., Keppel-Aleks, G., Allen, N. T., and Ayers, J.: TCCON data from Park Falls (US), Release GGG2014.R1, https://doi.org/doi:10.14291/tccon.ggg2014.parkfalls01.r1, 2017a.

Wennberg, P. O., Wunch, D., Roehl, C. M., Blavier, J.-F.v Toon, G. C., and Allen, N. T.: TCCON data from Lamont (US), Release GGG2014.R1, https://doi.org/doi:10.14291/tccon.ggg2014.lamont01.r1/1255070, 2017b.

Wennberg, P. O., Wunch, D., Roehl, C. M., Blavier, J.-F., Toon, G. C., and Allen, N. T.: TCCON data from Caltech (US), Release GGG2014.R0, https://doi.org/doi:10.14291/tccon.ggg2014.pasadena01.r0/1149162, 2017c.

Wu, L., Hasekamp, O., Hu, H., Landgraf, J., Butz, A., aan de Brugh, J., Aben, I., Pollard, D. F., Griffith, D. W. T., Feist, D. G., Koshelev, D., Hase, F., Toon, G. C., Ohyama, H., Morino, I., Notholt, J., Shiomi, K., Iraci, L., Schneider, M., de Mazière, M., Sussmann, R., Kivi, R., Warneke, T., Goo, T.-Y., and Té, Y.: Carbon dioxide retrieval from OCO-2 satellite observations using the RemoTeC algorithm and validation with TCCON measurements, Atmospheric Measurement Techniques, 11, 3111–3130, https://doi.org/10.5194/amt-11-3111-2018, https://www.atmos-meas-tech.net/11/3111/2018/, 2018.

Wunch, D., Toon, G. C., Blavier, J.-F. L., Washenfelder, R. A., Notholt, J., Connor, B. J., Griffith, D. W. T., Sherlock, V., and Wennberg, P. O.: The Total Carbon Column Observing Network, Philosophical Transactions of the Royal Society A: Mathematical, Physical and Engineering Sciences, 369, 2087–2112, https://doi.org/10.1098/rsta.2010.0240, 2011a.

Wunch, D., Wennberg, P. O., Toon, G. C., Connor, B. J., Fisher, B., Osterman, G. B., Frankenberg, C., Mandrake, L., O'Dell, C., Ahonen, P., Biraud, S. C., Castano, R., Cressie, N., Crisp, D., Deutscher, N. M., Eldering, A., Fisher, M. L., Griffith, D. W. T., Gunson, M., Heikkinen, P., Keppel-Aleks, G., Kyrö, E., Lindenmaier, R., Macatangay, R., Mendonca, J., Messerschmidt, J., Miller, C. E., Morino, I., Notholt, J., Oyafuso, F. A., Rettinger, M., Robinson, J., Roehl, C. M., Salawitch, R. J., Sherlock, V., Strong, K., Sussmann, R., Tanaka, T., Thompson, D. R., Uchino, O., Warneke, T., and Wofsy, S. C.: A method for evaluating bias in global measurements of CO_2 total columns from space, Atmospheric Chemistry and Physics, 11, 12 317–12 337, https://doi.org/10.5194/acp-11-12317-2011, https://www.atmos-chem-phys.net/11/12317/2011/, 2011b.

Wunch, D., Mendonca, J., Colebatch, O., Allen, N. T., Blavier, J.-F., Roche, S., Hedelius, J.v Neufeld, G., Springett, S., Worthy, D., Kessler, R., and Strong, K.: TCCON data from East Trout Lake, SK (CA), Release GGG2014.R1, https://doi.org/doi:10.14291/tccon.ggg2014.easttroutlake01.r1, 2017.

Zhang, Y., Gautam, R., Pandey, S., Omara, M., Maasakkers, J. D., Sadavarte, P., Lyon, D., Nesser, H., Sulprizio, M. P., Varon, D. J., Zhang, R., Houweling, S., Zavala-Araiza, D., Alvarez, R. A., Lorente, A., Hamburg, S. P., Aben, I., and Jacob, D. J.: Quantifying methane emissions from the largest oil-producing basin in the United States from space, Science Advances, 6, https://doi.org/10.1126/sciadv.aaz5120, 2020.